1968

Spacing of explosive charges

Calvin J. Konya

SPACING OF EXPLOSIVE CHARGES

BY

CALVIN JOSEPH KONYA, 1943

A

THESIS

submitted to the faculty of

THE UNIVERSITY OF MISSOURI - ROLLA

in partial fulfillment of the requirements for the

Degree of

MASTER OF SCIENCE IN MINING ENGINEERING

Rolla, Missouri

1968

Approved by

Ronald R. Rollins (advisor) Charles J. Haas

R. J. Bruzewski

ABSTRACT

It is generally believed that the spacing of simultaneously initiated collar primed multiple charges is not dependent on the charge length. The stresses generated by explosive charges have been assumed to propagate through a material in a cylindrical manner. This assumption implied that the stress generated in any plane along the charge diameter would have been uniform in magnitude and direction. A finite explosive velocity along with a conical stress wave causes the stresses near the collar to differ from those farther down the column. For this reason, the spacing of charges would be dependent on charge length.

An experimental technique using models was employed to investigate charge length and other spacing parameters. Materials with different properties were selected as models for the purpose of determining to what extent material's properties influenced the spacing.

This investigation showed that charge length was of extreme importance in the spacing of instantaneously initiated charges of short length. This could be attributed to decreased stress intensities in the collar region caused by noncoherent wave fronts in this region.

ACKNOWLEDGEMENTS

The author wishes to express his gratitude to Dr. Ronald R. Rollins and Professor Richard L. Ash for their advice during the course of this investigation. The author is also indebted to Professor Robert F. Bruzewski and Everett Ragan for their suggestions and assistance and to his wife, Patricia Konya for typing this thesis.

TABLE OF CONTENTS

Page

APPENDICES

LIST OF FIGURES

LIST OF TABLES

LIST OF PLATES

I. INTRODUCTION

Spacing and burden relationships for confined cylindrical explosive charges serve as the basis for the design of all blasting rounds. In surface blasting, length to burden (L/B) ratios vary from large diameter holes which have burdens and lengths which are almost equal, to small diameter holes which are very long compared to their burdens. Multiple explosive charges may vary considerably in the manner of initiation (collar priming, bottom priming and multiple priming) and with the time interval between initiation of adjacent holes. The mechanisms of spacings and fracturing between holes are fairly well understood, but there is no information available regarding the influence of charge length on spacing and very little on the reinforcing effects in the burden dimension of instantaneously initiated adjacent charges. It was the purpose of this investigation, therefore, to observe the interrelation of the spacing, depth of burial and charge length on collar primed instantaneously initiated cylindrical charges.

In situ testing would require reasonably large scale blasts, the results of which would be difficult to interpret and analyze accurately. They would also be expensive and require the movement of a considerable amount of broken material. In order to keep a closer control on the testing and collect the greatest amount of reliable data, a laboratory study was undertaken.

Mild Detonating Fuse (MDF) of the 10 and 20-grain strengths were chosen for the explosive. MDF was chosen after considering other explosives because of its high velocity and density, small critical diameter, high energy release, uniformity of reaction rate and explo-

sive pressure and safety and ease in handling.

Studies were made first in Plexiglas to observe internal fracture patterns. The influence of the material's properties on the spacing was investigated by conducting tests on samples of cement mortar and Jefferson City Dolomite. The physical properties of these materials differ widely in grain size, Poisson's ratio, compressive and tensile strengths, density and sonic velocities. All the materials were easily cut, formed and drilled. Although this investigation was basically qualitative, compressive, tensile and sonic velocity tests were conducted on the materials prepared in the laboratory so that the material's properties could be defined with some degree of accuracy.

II. EFFECTS OF SPACING GEOMETRY

Optimizing spacing of multiple charges is the process by which the energy released from an explosive reaction is utilized in the most efficient manner to move the maximum amount of material of a predetermined size distribution. Multiple initiation of blastholes regardless of the type of pattern employed can be broken down into two basic types, simultaneously fired adjacent holes which reinforce one another to some degree, and separately fired adjacent holes fired at some delay (3,4,18,19).

A. Effects of Spacing

If the spacing between blastholes is excessive, in the case of instantaneously initiated adjacent charges, humps and toes remain in the floor between blast holes and horizontal cratering occurs (Fig. 1). As the spacing is reduced the area between holes becomes fractured and fragmentation of two relative sizes results. Small particle size results in the crater area of the single charge while boulders occur between the holes. As the spacing is further decreased and the optimum spacing approached, the maximum volume of uniformly sized material is reached. If the spacing is further reduced, a number of undesirable effects are observed. Premature shearing results between holes which can cause a low velocity explosive such as a blasting agent to extinguish itself due to a loss of confining pressure. Premature loss of gases due to premature shearing will result in vertical cratering, overbreak (crushing between holes and boulders resulting in the burden

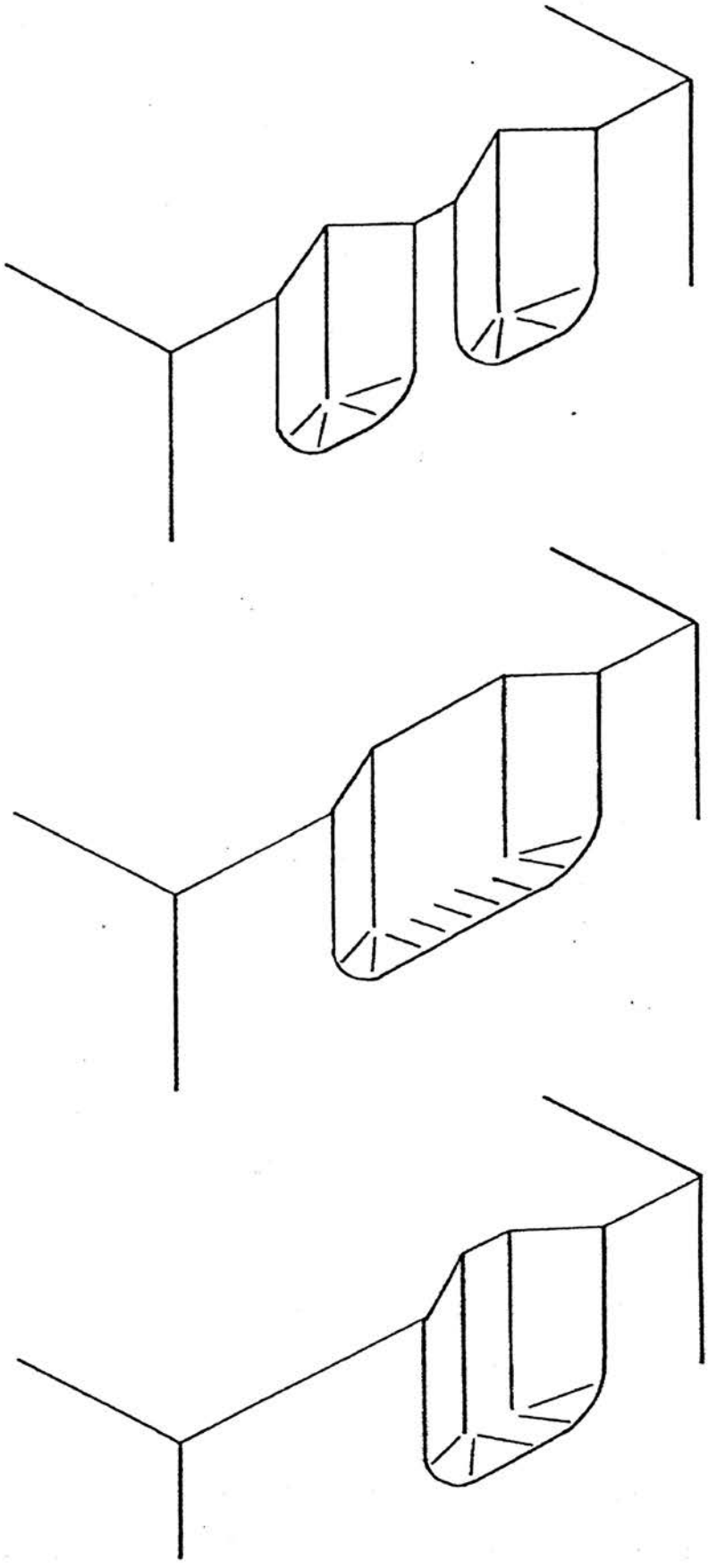

Figure 1. Horizontal Craters

dimension) and toes at floor level.

Two basic types of benches are observed in surface blasting (Fig. 2). Blasting with a closed bottom is by far the most prevalent and can be seen in almost any quarry. The open bottom condition is used by many coal stripping operations and in this case the borehole does not enter the coal seam. It is also interesting to note that in many of these large stripping operations, large diameter boreholes are utilized and the length (L) of the borehole may not be much greater than the burden (B). In many cases the L/B ratio is between 1 and 3.

B. Fracture Mechanisms

The shock wave due to the detonation pressure is considered to have little effect on fracturing under normal field conditions (3, 13 19). Fracturing seems to be directly related to quickly applied high pressures resulting from explosive reactions. The result is that two types of body motions are developed and propagated in the form of compressional (P) and shear (S) elastic waves. These two wave velocities are related by Poisson's ratio, μ, provided that μ is neither negative nor does it equal or exceed .5. The faster of the two waves is the P wave, therefore, it is the first to arrive at an interface. When a P wave strikes an interface between two materials, in general, four stress waves are generated. Two of these waves are refracted and two are reflected back into the material. The angle of incidence of the compressional wave and the characteristic impedances of the materials control the magnitudes and directions of the refracted and reflected waves (5,11,17). In normal blasting, under most field conditions, little

a. Vertical Section of Open Bottom Bench

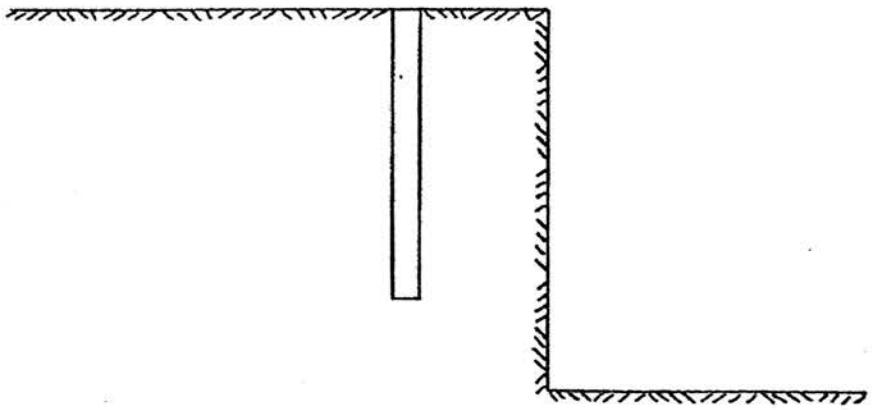

b. Vertical Section of Closed Bottom Bench

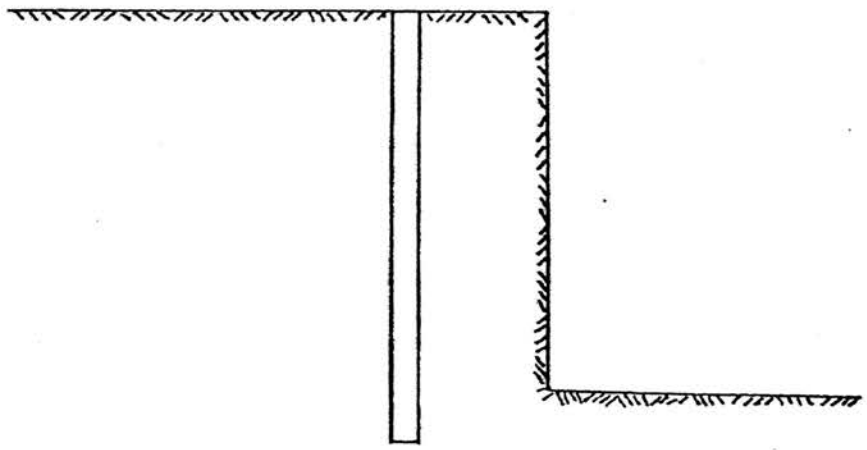

Figure 2. Bench Forms for Surface Blasting

energy would be lost due to refraction at a rock-to-air interface and, therefore, only the reflected stresses are usually considered (17).

In the past, it was generally believed that a cylindrical compressive wave (Fig. 3) emanated from the long length charge. Measurements of strain waves have proved that this is not the case (25). This would be the case if either the explosive had infinite velocity or if many primers would be evenly spaced along the explosive column and detonated simultaneously. It has been shown that since the explosive does not have an infinite velocity, a collar primed long length charge will form a conical wave (Fig. 4) if the detonation velocity of the explosive is greater than the wave propagation velocity of the rock (3). The apex of this wave is in the direction opposite that of primer placement. At a distance from the top interface, the wave front will assume a conical shape with one half of the apex angle equal to the arcsine of the P wave velocity divided by the velocity of the explosive ($\sin^{-1} \frac{V_p}{V_e}$) (Fig. 5).

With the assumption of the cylindrical compressive wave, the stress reinforcement due to adjacent simultaneously fired charges was considered to be only in the plane of the charge diameter, and the reinforcement was assumed only between the holes. The overall effect of spacing was determined by geometrically balancing the stresses in this plane. The two basic, well-known geometric spacing relationships are shown in (Fig. 6) and suggest spacings in the range of 1.4 and 2 times the burden. Many empirical formulas are available for burden calculation (1,3,13,16,19,20,22,24). These will not be discussed, but the fact will be noted that in some cases, it is suggested that the burden

a. Vertical Section

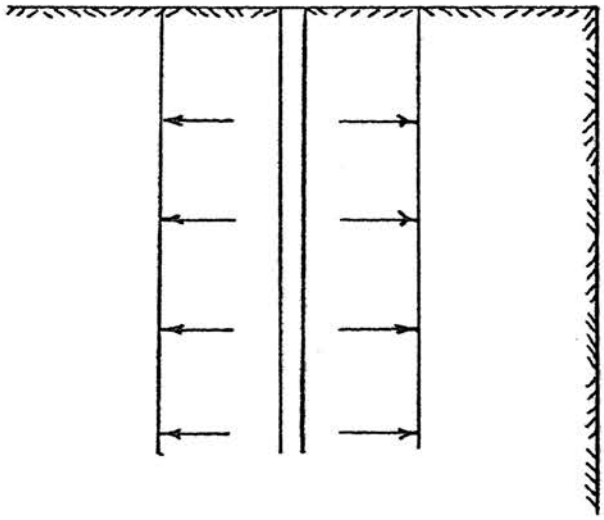

b. Plan View at Top Free Surface

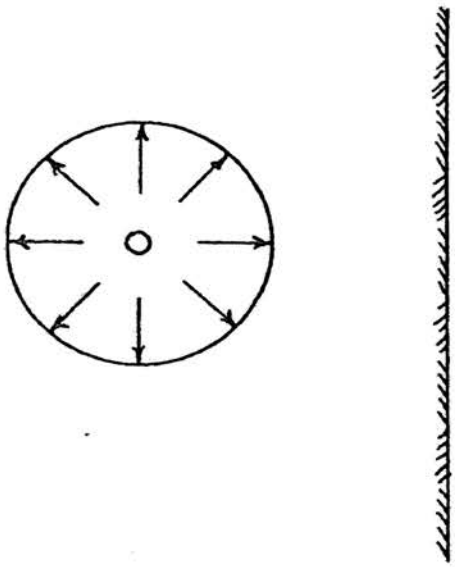

Figure 3. Cylindrical Compressive Wave Form Emanating from a Long Length Charge

a. Vertical Section

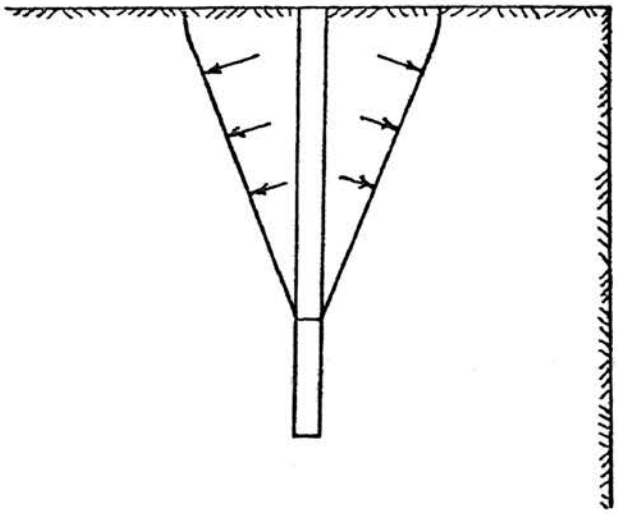

b. Plan View at Top Free Surface

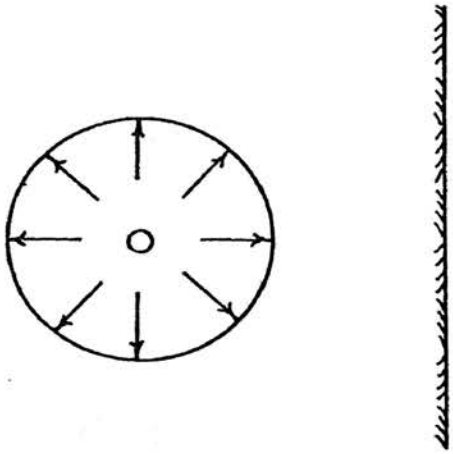

Figure 4. Conical Compressive Wave Form, Moving Down a Long Column of Detonating Explosive

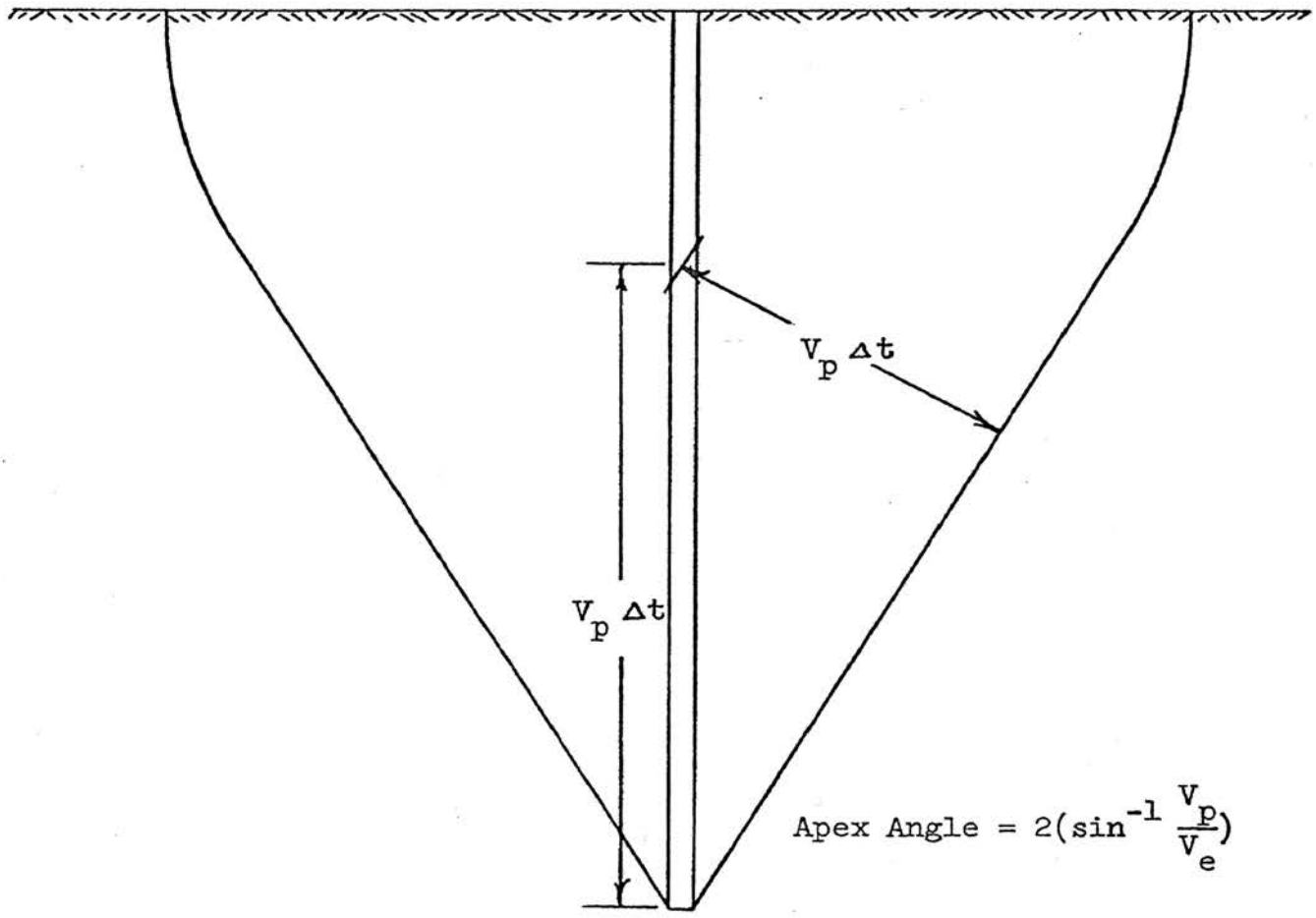

Figure 5. Angle of Conical Wave

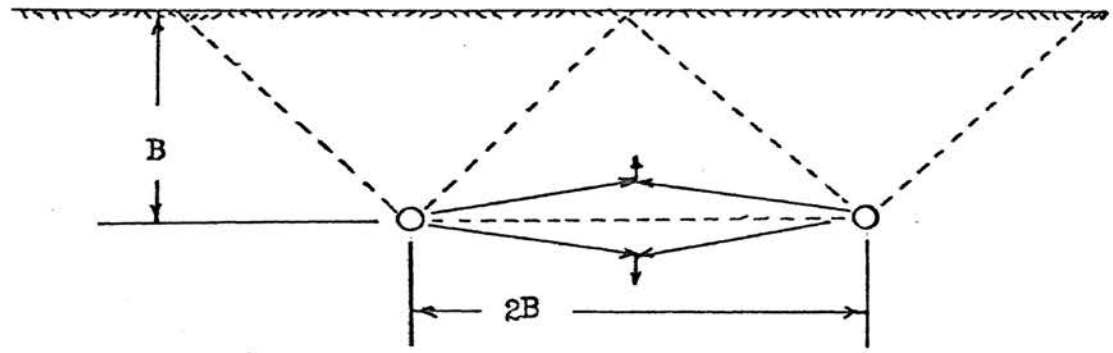

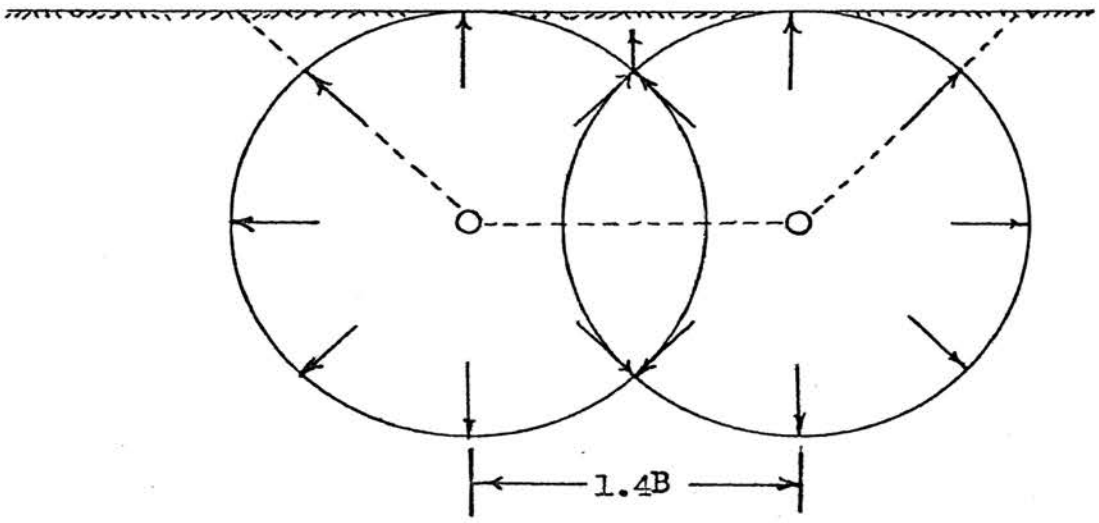

Figure 6. Spacing Relationships Determined by Geometrically Balancing Stresses in the Plane of the Charge Diameter.

is independent of the spacing, and that the optimum burden for a material can be found by exploding single charges at varying distances from the face. The burden is chosen as the distance which gives the type of fragmentation desired and removes the material along the entire length of the charge.

III. EXPERIMENTAL PROCEDURE

A. Model Preparation

A systematic approach was necessary to work with a problem such as spacing. The selection of control parameters and data collection could not be left to haphazard methods. For this reason, it was not advisable to use random observations on primary quantities (Appendix II., Eq. (1). Such observations would have been time consuming, difficulty could have resulted in relating quantities of more than three independent variables and false conclusions could have been reached. For this reason, this problem was analysed by dimensional analysis using an equation (Appendix II., Eq. (2)) which resulted in the determination of similitude ratio which gave the research direction and assisted in arriving at valid conclusions (21). To eliminate as many variables as possible, the open bottom bench condition was chosen, and the effects of stemming were eliminated by loading the holes completely to the collar.

The effect of geometry and material's properties could best be studied by selecting at least three materials of different physical characteristics. Plexiglas, cement mortar and Jefferson City Dolomite were selected as the experimental media, not only for the above reasons, but also because of ease in model preparation. Other investigators had used these materials and comparison with other data was available. The Plexiglas could be purchased in large sheets and cut to the desired model size. Mortar required mixing and casting in molds. The dolomite was locally available and needed only to be cut.

1. Choice of Model Size and Explosive

Plexiglas models varied as to their dimensions, except for that of width, which was fixed at 4 inches, the maximum thickness available. For large burdens and large L/B ratios, the model size was chosen as 7 x 12 x 4-inches while for short L/B ratios and small burdens, the size was reduced to approximately 7 x 7 x 4-inches. The models used to completely eliminate the effects of gas pressure were 1/2 inch thick and their length and width were dependent on the L/B ratio used. For L/B = 1, models were about 3 x 3 x 1/2-inch. Mortar was cast in one foot cubes and also in 6 x 12 x 12-inch blocks. Smaller blocks were cored and tests were run to determine the material's properties. Dolomite samples were prepared by cutting blocks approximately 9 x 9 x 18-inches.

The 20-grain MDF was not used as the explosive for the spaced charges, because its greater power would have required a larger model size. MDF of the 10-grain variety was used in models of either single charges or those with spacing other than zero. For a spacing of zero, 20-grain MDF was used to simulate a double charge in the same borehole. (Table 1).

2. Sample Preparation

Plexiglas models were prepared from a 4 x 24 x 48-inch sheet manufactured by the Rohm and Haas Company. Cutting was accomplished by means of a power hacksaw which was found more efficient than a wood table saw. Models were then finished by milling the sawed surfaces on a horizontal boring mill.

Table 1

Explosive's Properties (9,12)

Type	PETN (gr/ft)	Diameter of Explosive (in.)	V_e(fps)	Explosion Pressure (psi)
MDF A-10	10	.047	24,000	1,760,000
MDF A-20	20	.072	22,000	1,760,000

Mortar models were prepared in two batches using two parts (by weight) Portland cement, one part water and four parts Ottawa sand (a fine grained, uniformly sized sand). A power driven paddle-type rotary mixer was used to mix the ingredients. After alternately loading small quantities of the ingredients and mixing a full batch for 30 minutes, the mixture was poured into pre-fabricated molds of the desired size. The molds were made of .75-inch plywood. The rim and groove type of mold was used and permitted casting of two, cubic foot, blocks and two, 12 x 12 x 5.875-inch, blocks (6). The mold was greased on the inside to prevent sticking. The molds were vibrated for 45 seconds to eliminate air bubbles. Specimens were allowed to consolidate for 24 hours, after which they were removed from the molds and allowed to cure for 7 days at 68 degrees Fahrenheit and 100% relative humidity.

B. Determination of Physical Properties

Approximate physical properties of some of the materials used in this investigation could be found in the literature. Mortar models consisted of a type of sand not normally used because of its uniform grain size and high cost. For this reason, tests were conducted to determine the properties of this material.

1. Density

Each mortar model was measured to the nearest 1/16-inch and weighed to the nearest 1/10 pound. These values were compared with values in the literature (See Appendix VI.).

2. Sonic Velocity

Characteristic longitudinal wave velocities were determined by using the sonic pulse technique. The instrumentation was first used by J. H. Deatherage and is completely described in his M.S. Thesis (10). This technique utilizes two piezoelectric transducers. One transducer, when connected to a pulse generator, acted as a miniature sending unit. An electrical signal sent by the pulse generator was changed to a mechanical pulse by the transducer and sent through the specimen as a longitudinal wave. The mechanical signal was picked up by the second transducer on the opposite side of the specimen and changed into an electrical pulse which was fed into an oscilloscope along with a synchronizing pulse. Travel time of the pulse through the specimen could be recorded to the nearest half microsecond. By knowing the travel time and the length of the specimen, the longitudinal wave velocity could be calculated (Appendix III.).

The shear-wave velocity was more difficult to determine because reflected longitudinal waves and Rayleigh waves were also present on the oscilloscope trace. For this reason, large mortar samples were used to eliminate reflected longitudinal waves. The shear waves could then be determined because the shear-wave arrival time was quicker than that of the Rayleigh waves (Appendix III.).

3. Compressive Strength

The test procedure employed in determining the compressive strength of the mortar was similar to that used by ASTM for the testing of building stone. Apparatus used to conduct this test was a diamond core drill, a diamond saw, a power finishing grinder and a 120,000 pound hydraulic testing machine. Cores of 2.125-inches in diameter

were cut to lengths of approximately 4.25 inches. Sample ends were ground on the finish grinder so that they were parallel to one another and perpendicular to the sides. After careful alignment in the hydraulic testing machine, the cores were loaded at a uniform rate until failure occurred. The load at failure and the cross-sectional area are all that are required to calculate the compressive strength (Appendix IV.).

4. Tensile Strength

The apparatus necessary to conduct the Brazilian tensile test was the same as that used for the compressive strength. Specimens were 2.125 inches in diameter and approximately 2.125 inches long. Cores were loaded on a line on the circumference and along the length of the specimen. Blotting paper was used to distribute the load over the entire line rather than on the high spots. The loading rate was closely controlled. Tensile strength could be calculated from the following equation (Appendix V.):

$$\text{Tensile Strength} = \frac{2P}{3.14DL}$$

where

P is the load at failure

D is the core diameter

L is the core length

A summary of the material's properties can be found in Table 2.

C. Placement and Initiation of Explosive Charges

Charge holes in the Plexiglas were drilled with a 6-inch long

Table 2

Material's Properties (9,10,14,15,23)

Material	V_p (fps)	V_s (fps)	σ_c (psi)	σ_t (psi)	τ (psi)	Sgr	Z (lb-sec/ft^3)	μ
Air	1,100	---	---	---	---	.012	2.6	---
Dolomite	14,600	8,600	9,000	220	7,500	2.5	71,700	.27
Granite	16,000	9,300	30,000	3,000	15,000	2.5	77,500	.25
Hydrostone	11,000	6,600	7,200	2,000	6,000	1.7	36,600	.18
Mortar	13,000	8,400	7,100	360	1,600	2.2	56,700	.15
Plexiglas	8,800	3,500	11,000	7,500	5,400	1.2	21,400	.40
Water	4,750	---	---	---	---	1.0	9,200	.50

.125-inch diameter drill bit. Mortar and dolomite were drilled using a 5-inch tungsten carbide tipped, straight shank, tapered length, Type 1120 Chicago Latrobe bit. The samples were all drilled in a standard drill press. A stream of compressed air was direct against the drill bit to help bring up cuttings and to cool the bit.

The models required varying lengths of explosive charges depending on the burden and L/B ratio. Care was taken to cut the two charges to the same length. They were detonated simultaneously using a No. 6 blasting cap, the MDF was placed in the blasthole and the protruding ends were aligned and brought together. A single cap would initiate both at the same position along both charges. Hydraulic oil was used in the borehole to insure coupling. Samples were protected from the effects of the blasting cap by a steel plate placed between the cap and the specimen. The plate was made of a .125 x 10 x 10-inch steel plate with a pair of .125-inch holes drilled to permit the passage of the explosive. Specimens were placed within a blasting chamber constructed of steel and lined with 3 inches of wood and detonated with a 10 cap twist type blasting machine.

Since the Plexiglas specimens could only be purchased with a maximum thickness of 4 inches, it was necessary to submerge the back of the specimen in water about three inches to prevent the sample from splitting in half when using long charges. The impedance of the water being more nearly that of the Plexiglas allowed more energy to be refracted instead of being reflected back into the sample as would result using a Plexiglas-air interface.

IV. DISCUSSION OF RESULTS

To further assist in the evaluation of the effects of various spacing parameters, six specific quantities were measured. These included the following: charge length, spacing in inches, the fraction of the total charge length broken out, angle x measured in the plane of the charge diameter (Fig. 7), angle y measured in the plane of the charge length (Fig. 8) and the crater form which indicated whether the energy was sufficient to completely break between the holes (Fig. 9). This study of spacing was not related to the size distribution of the material broken by the explosive. For this reason, it must be emphasized that the criteria of failure of a specific spacing was if either the entire charge length was not broken out, or if the material between holes was not completely broken out.

As previously discussed in Chapter II, the compressive wave generated by the MDF was conical in nature except in the collar region. The wave form changed in this region because noncoherent wave fronts were formed, and the energy from the explosive reached the free surface as a series of weak pulses rather than one strong pulse (Fig. 10). For this reason, it would seem reasonable to assume that for single or delayed charges in low L/B regions that smaller burdens would have to be employed. This same phenomenon also effected the spacing of charges in low L/B regions. Due to the noncoherent waves generated in the collar region, the spacing between charges was greatly reduced, and charge length was a definite factor in the design of low L/B ratio blasts (Fig. 11). Figures 12, 13 and 14 (in Plexiglas, mortar and dolomite, respectively) show the results of tests conducted to establish

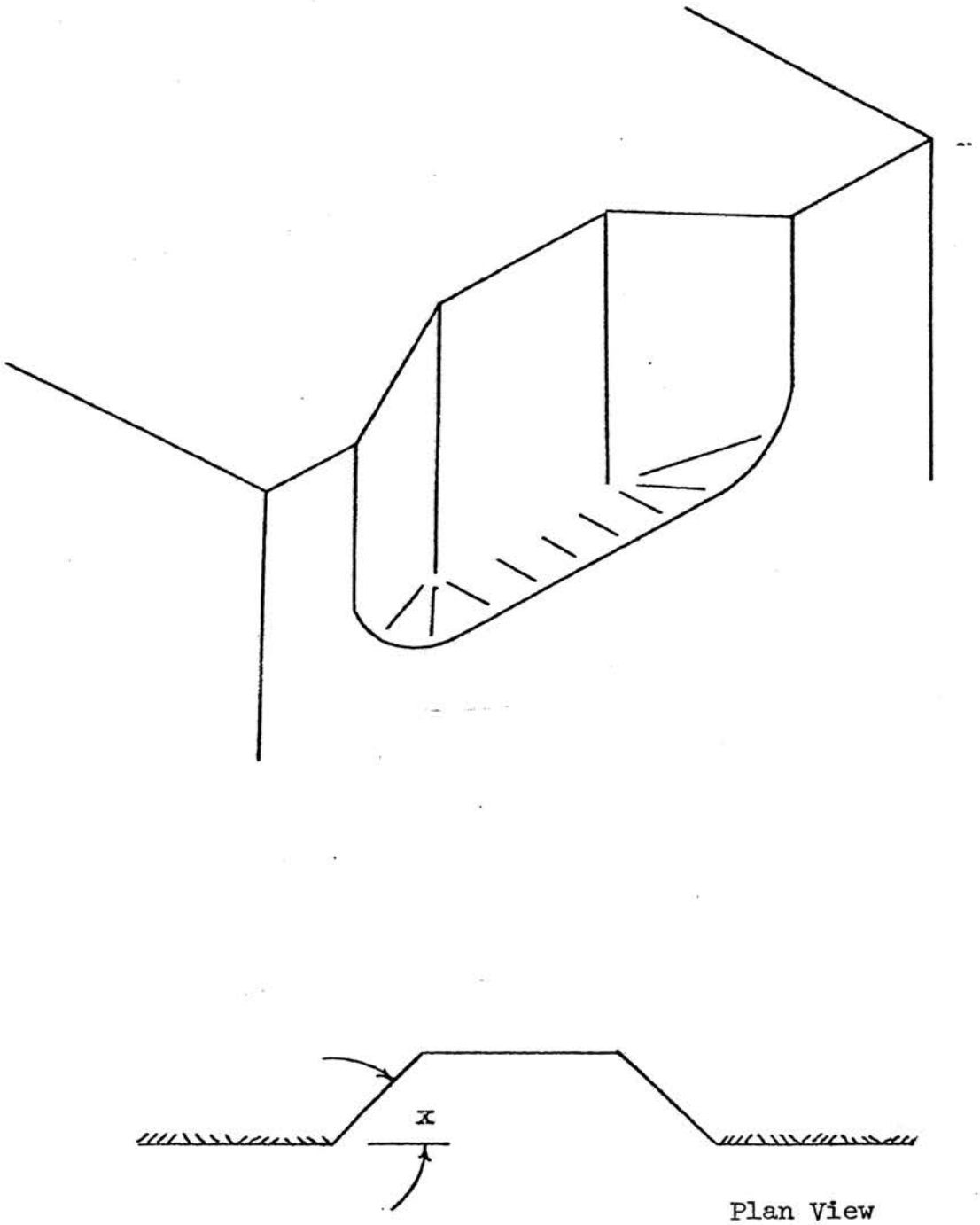

Figure 7. Crater Angle x

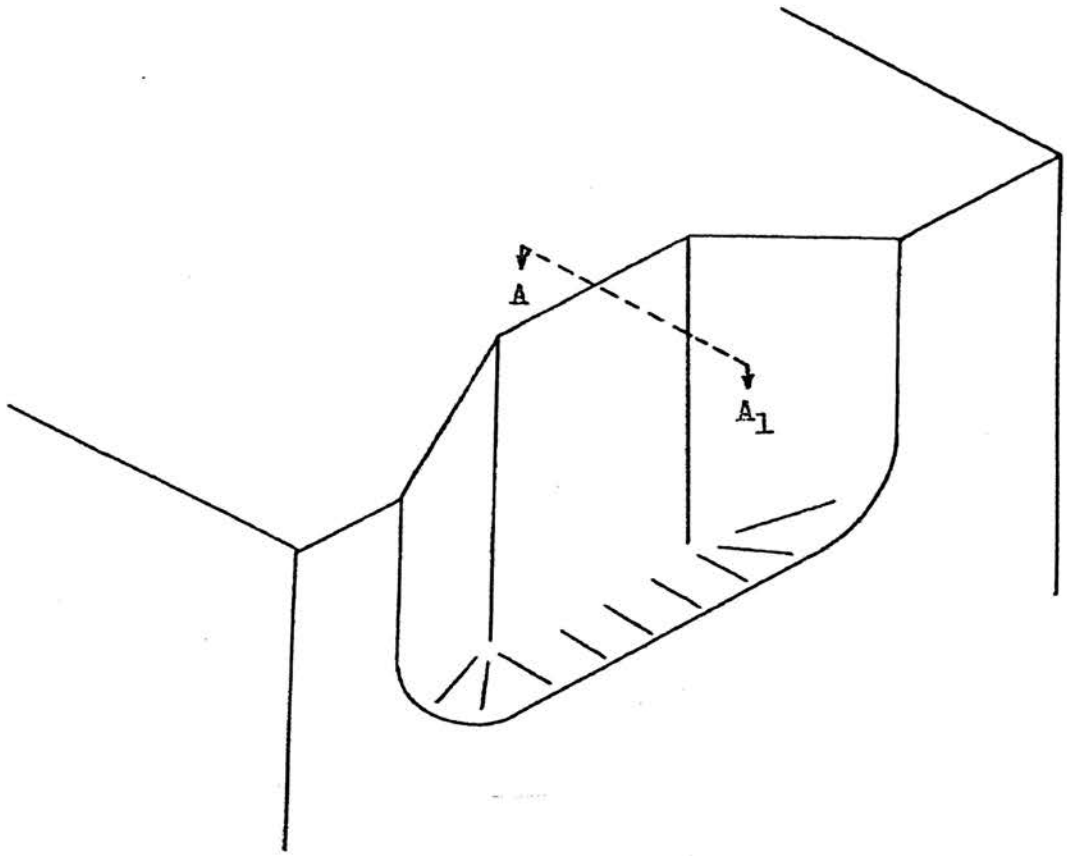

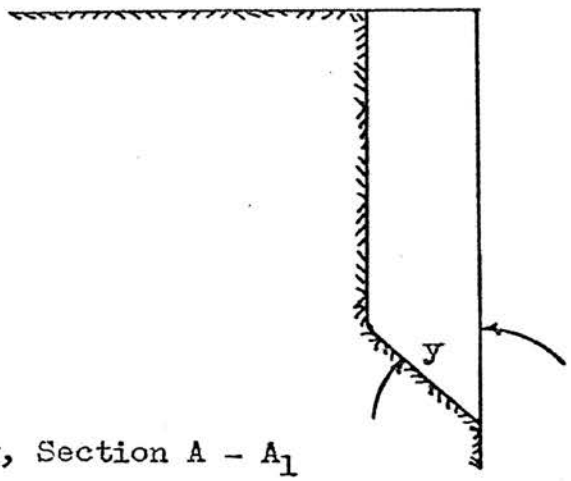

Vertical View, Section A - A_1

Figure 8. Crater Angle y

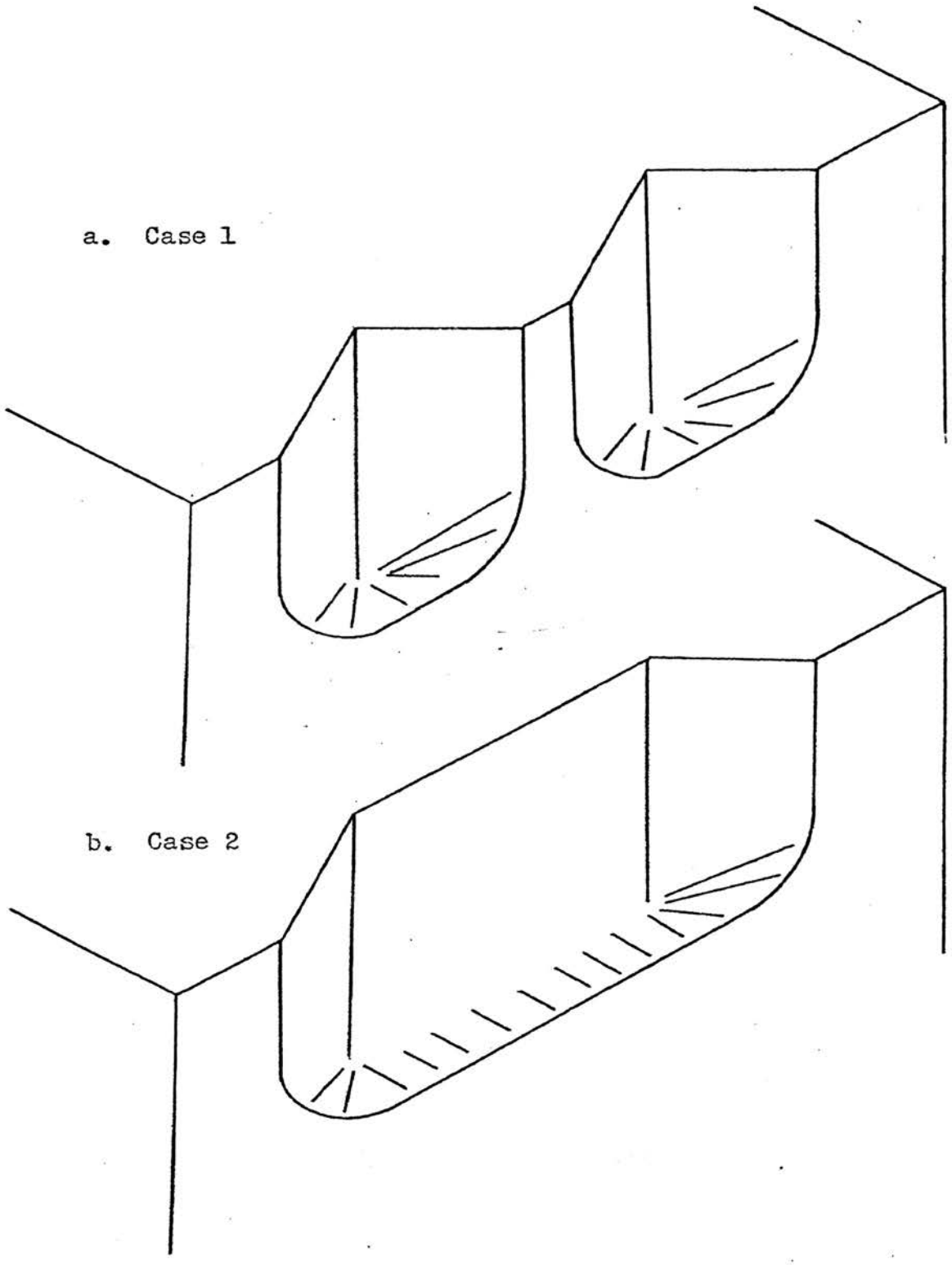

Figure 9. Crater Forms

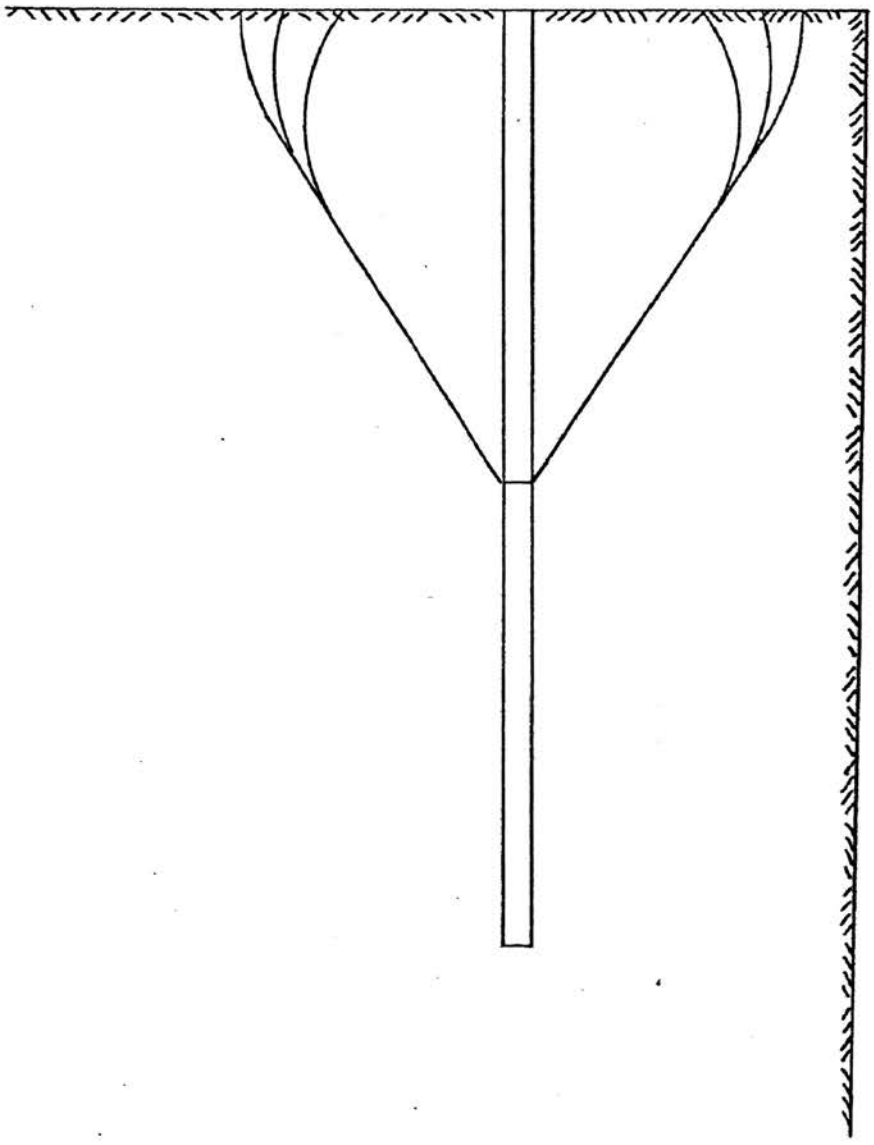

Figure 10. Noncoherent Wave Fronts in Collar Region

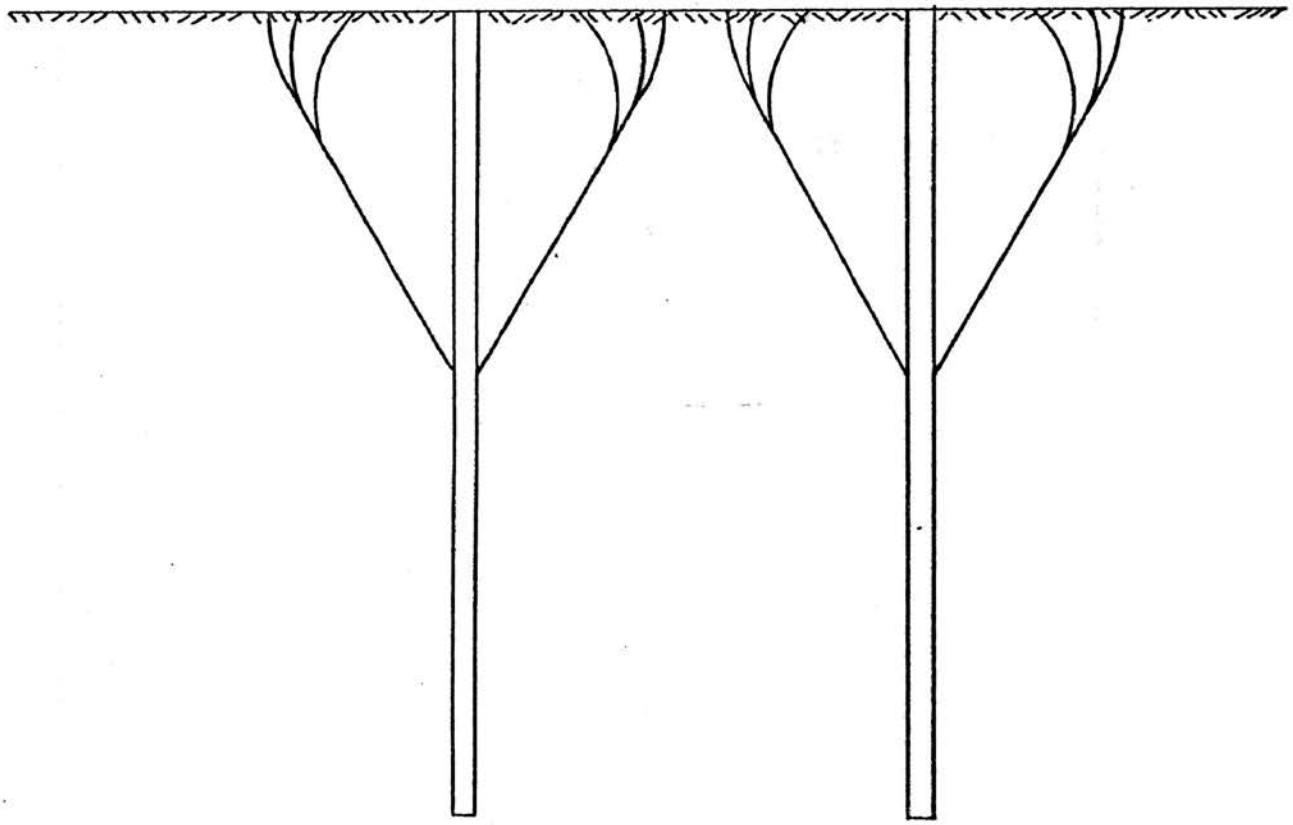

Figure 11. Noncoherent Wave Fronts between Two Simultaneously Initiated Charges

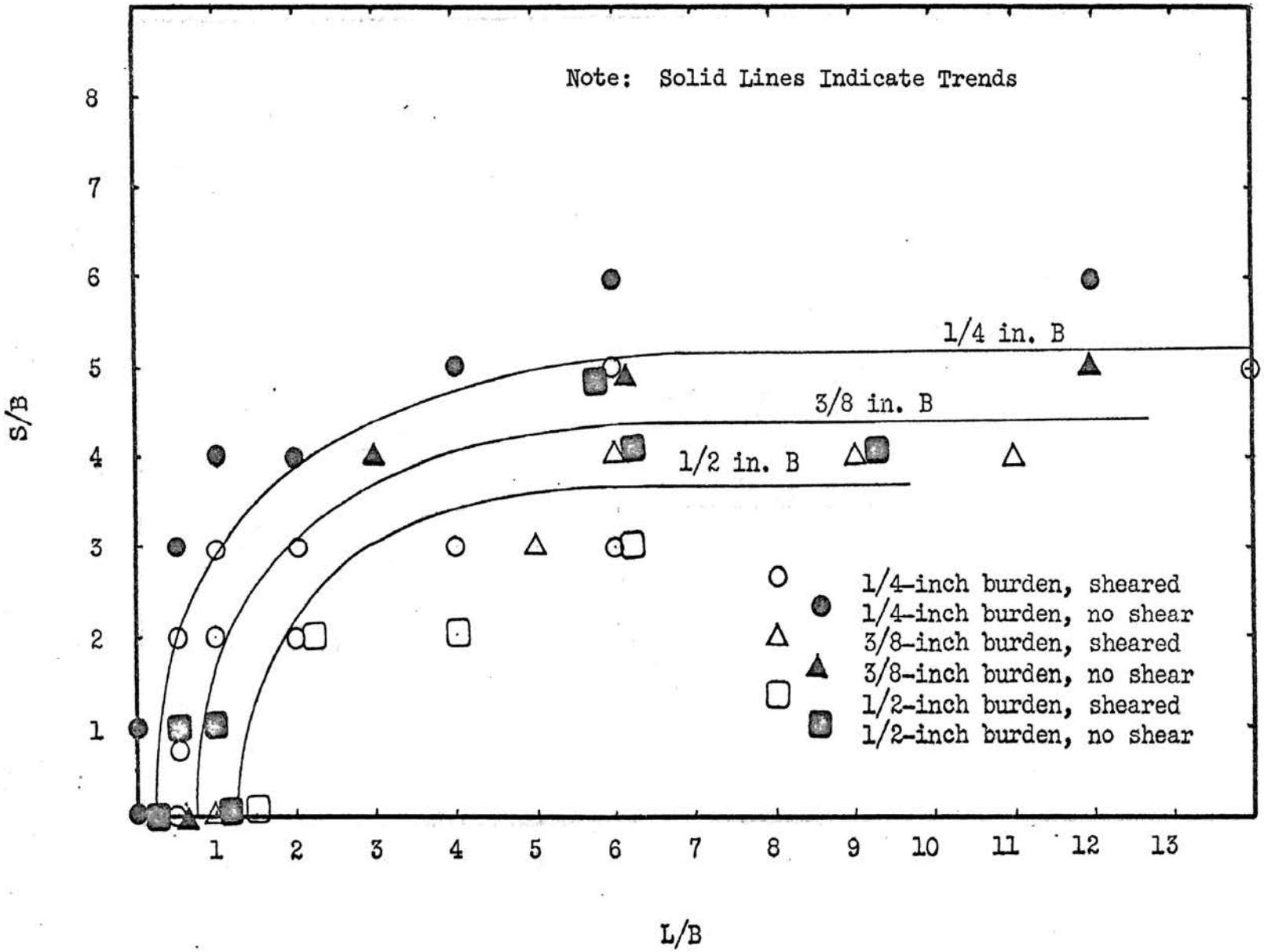

Figure 12. Explosive Spacing/Burden vs. Charge Length/Burden for Plexiglas

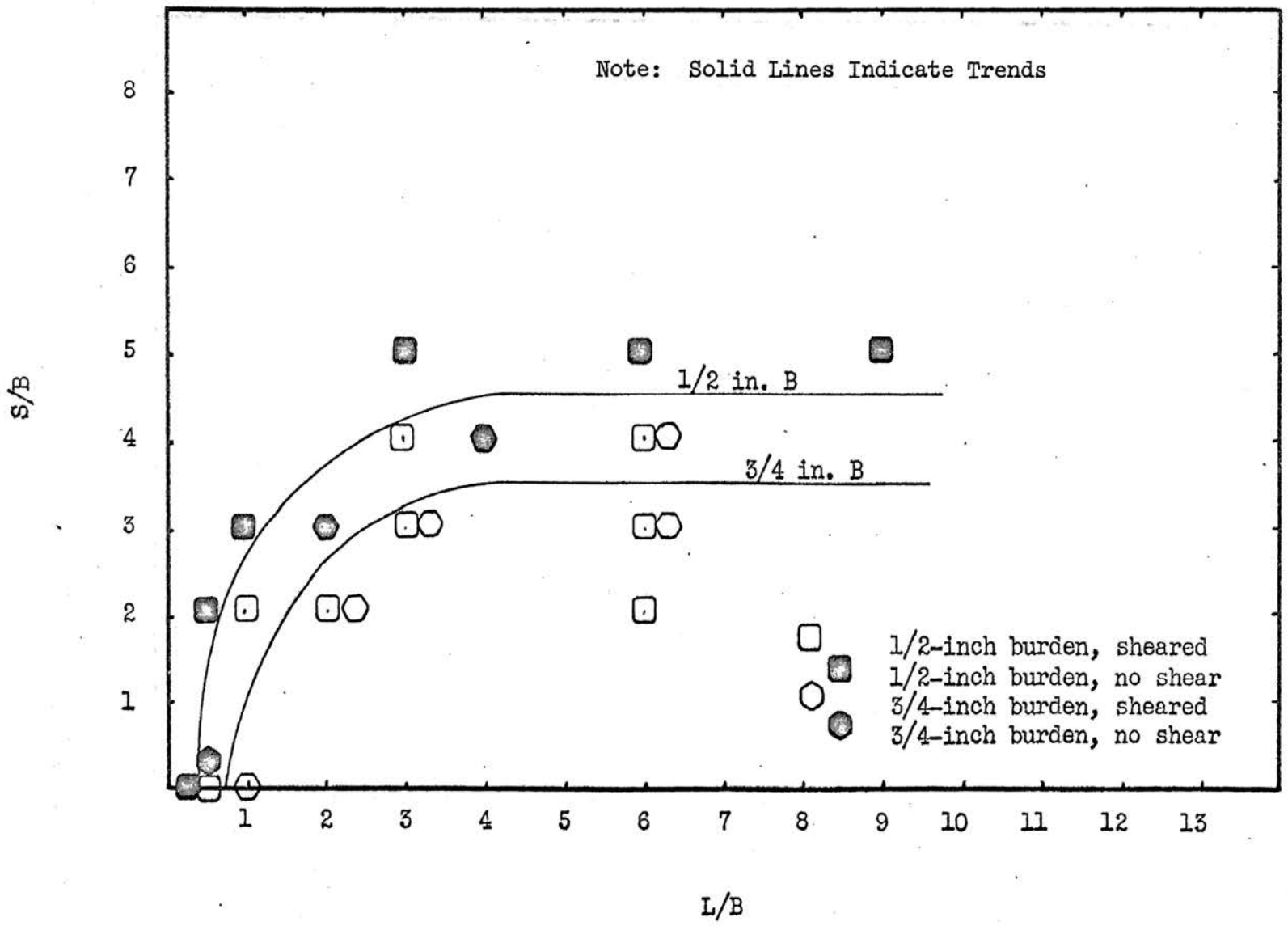

Figure 13. Explosive Spacing/Burden vs. Charge Length/Burden for Mortar

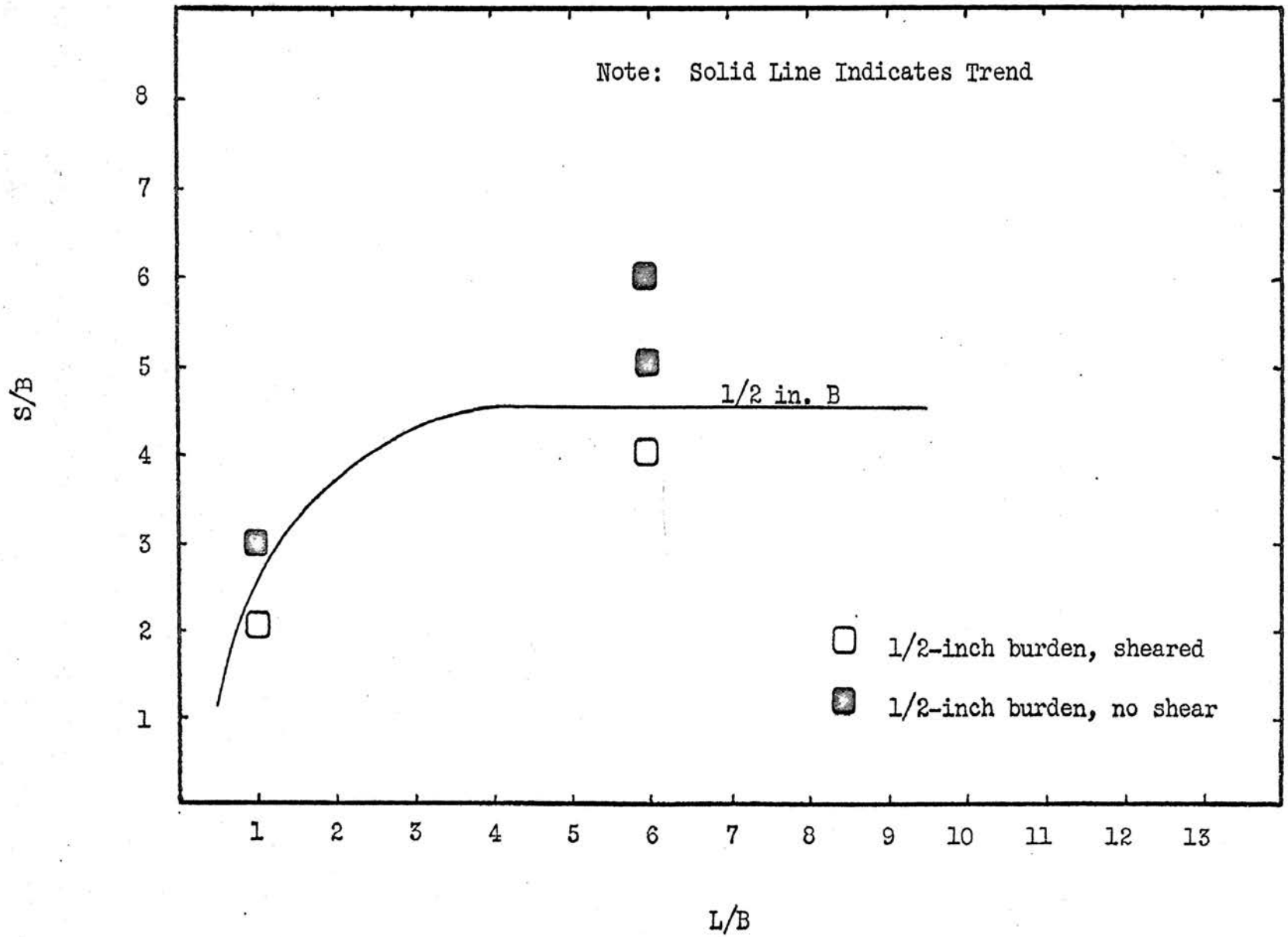

Figure 14. Explosive Spacing/Burden vs. Charge Length/Burden for Dolomite

the effects of charge length on spacing. These figures are plots of spacing divided by burden vs charge length divided by burden.

The graphs were drawn to best fit the experimental data. The small circles represented the tests conducted on the 1/4-inch burden, the triangles were 3/8-inch burden, the squares were 1/2-inch burden and the hexagons were 3/4-inch burden shots. The dark symbols represented the condition when the material failed to break between the holes while the clear symbols indicated complete breakage between the blastholes. The results in mortar and dolomite were very much alike while the curves obtained for Plexiglas were similar, but a smaller spacing was blasted using the same burden. This seemed reasonable because the Plexiglas had much higher shear and tensile strengths than either the mortar or dolomite. A larger maximum burden could be used in the mortar and dolomite for the same reason. These three graphs show that in low L/B ratio blasting, the spacing is reduced and a lesser amount of material is broken per pound of explosive used. The explosive could be used more efficiently by drilling smaller holes with small burdens while holding the bench height constant. If the bench height is variable, a longer bench would allow an increase in spacing for large diameter holes.

A series of .5-inch thick plates of Plexiglas were used to determine the effects of unconfined charges. Short lengths of 10-grain MDF (L/B = 1) were laid and detonated on the surface of the plates with direct contact only along the diameter of the charge. Plate I shows that very little fracturing occurred. Plate II shows the effects of a similar charge, the only difference being that the L/B ratio was equal to 2. Fracture patterns in the collar region of both plates

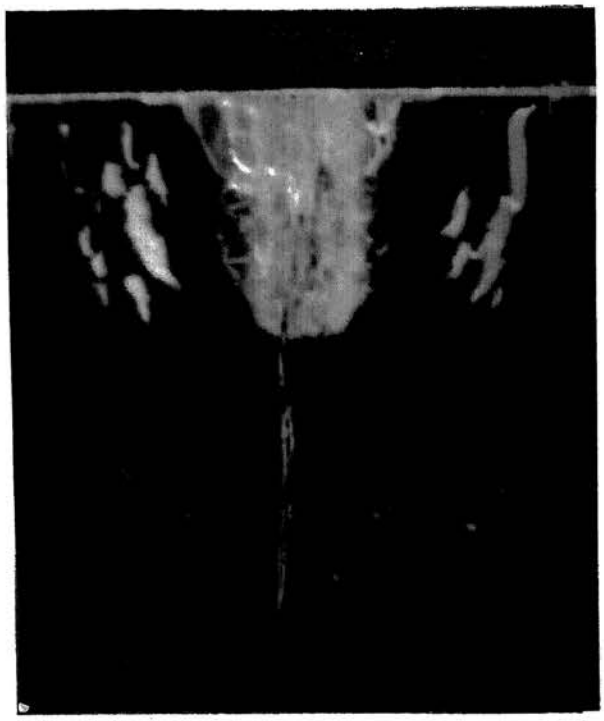

Plate I. Unconfined .5-inch long 10-grain MDF detonated on .5-inch Plexiglas Plate.

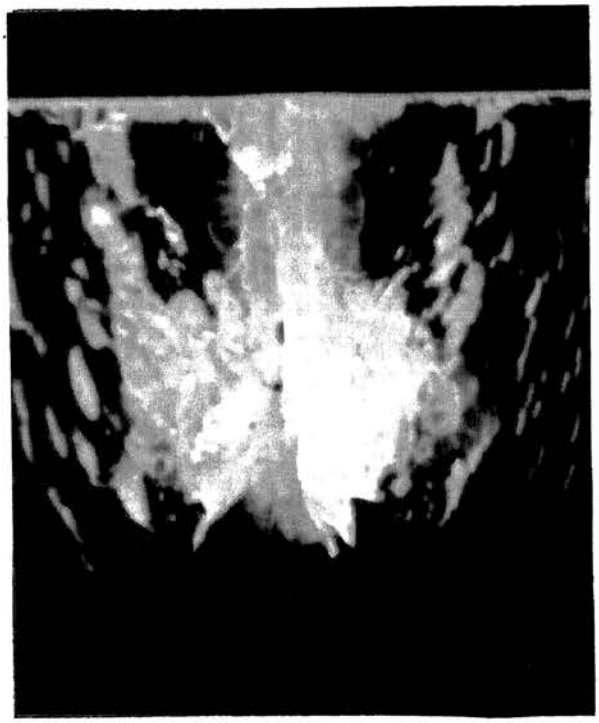

Plate II. Unconfined 1-inch long 10-grain MDF detonated on a .5-inch thick Plexiglas Plate.

are almost identical. As the charge length increased, the fracture intensity also increased to a point, beyond which it remained constant. Noncoherent wave fronts in the collar caused a lesser amount of fracturing in this region.

Figures 15 through 18 show the effect of spacing on the volume of material broken. The crater volumes were calculated using the equations in Appendix VII. Each material seemed to have a characteristic Spacing/(Charge Weight)$^{1/3}$ where the volume was the greatest regardless of the burden. Linear distance divided by (Charge Weight)$^{1/3}$ and volume of broken material divided by charge weight was used in Figures 15 through 17. This type of plot is a direct measure of the efficiency of the explosive in respect to a particular parameter which in this case was spacing. The 1/3 power was used in this type of scaling to account for energy dissipation in three dimensions and the final results were expressed on the unit energy basis. This method offered comparability of materials if all other parameters were held constant (7,8). The peaks in these curves showed the point where the scaled spacing gave the maximum volume of broken material.

Other effects of material's properties on spacing can be seen in Figures 19 and 20. Figure 19 is a plot of volume divided by charge weight vs log burden divided by (Charge Weight)$^{1/3}$. This plot would be the same for all materials if the angles of breakage (angle x, angle y) were constant. The effect of the high tensile strength of Plexiglas can be seen in Figure 20. Since the shear strength is less than the tensile strength, this material sheared easily between blastholes. In the small burden range, the spacing could be increased to better than five times the burden.

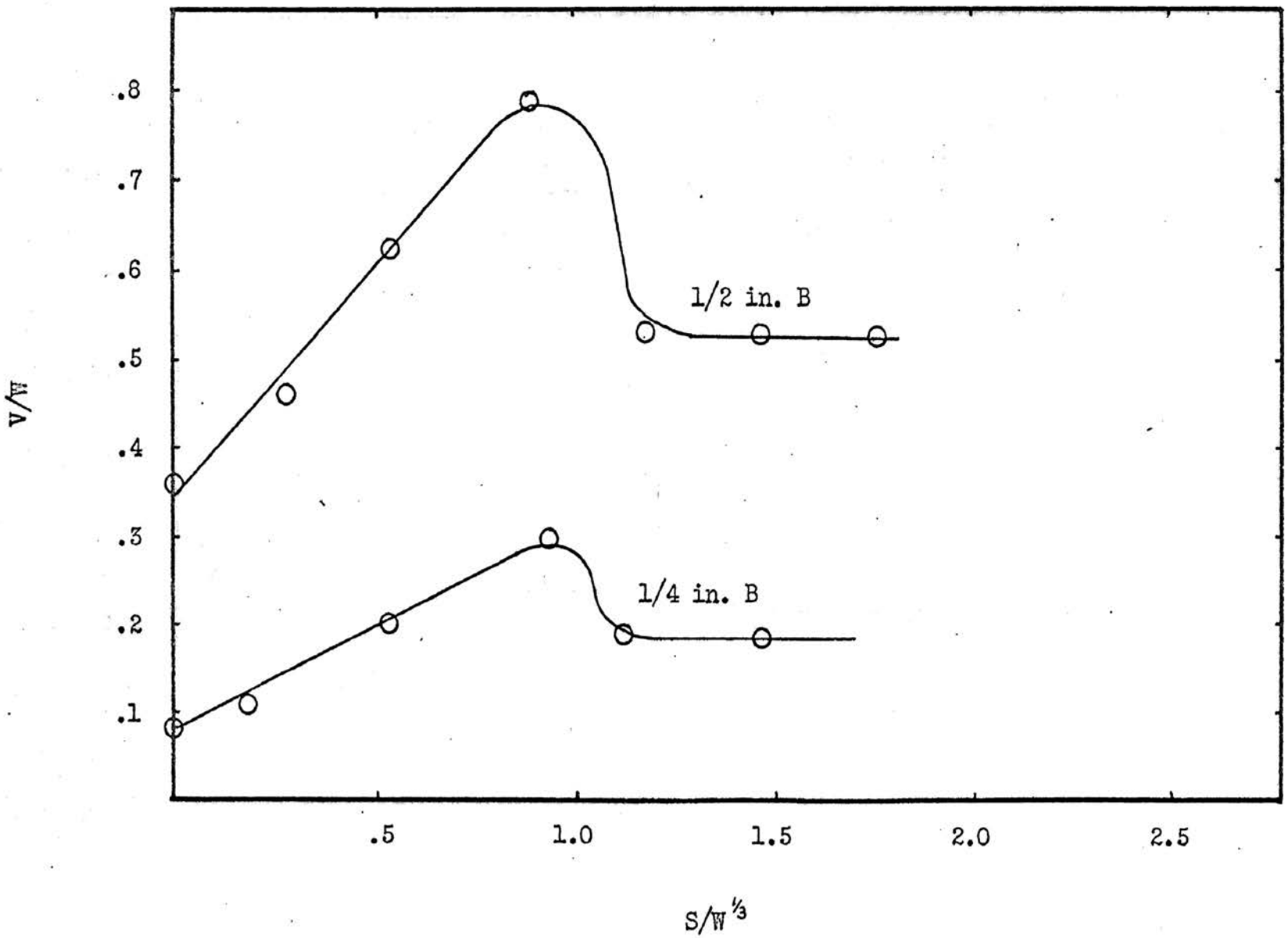

Figure 15. Crater Volume/Charge Weight vs. Explosive Spacing/(Charge Weight)$^{1/3}$ for Plexiglas (L/B = 6)

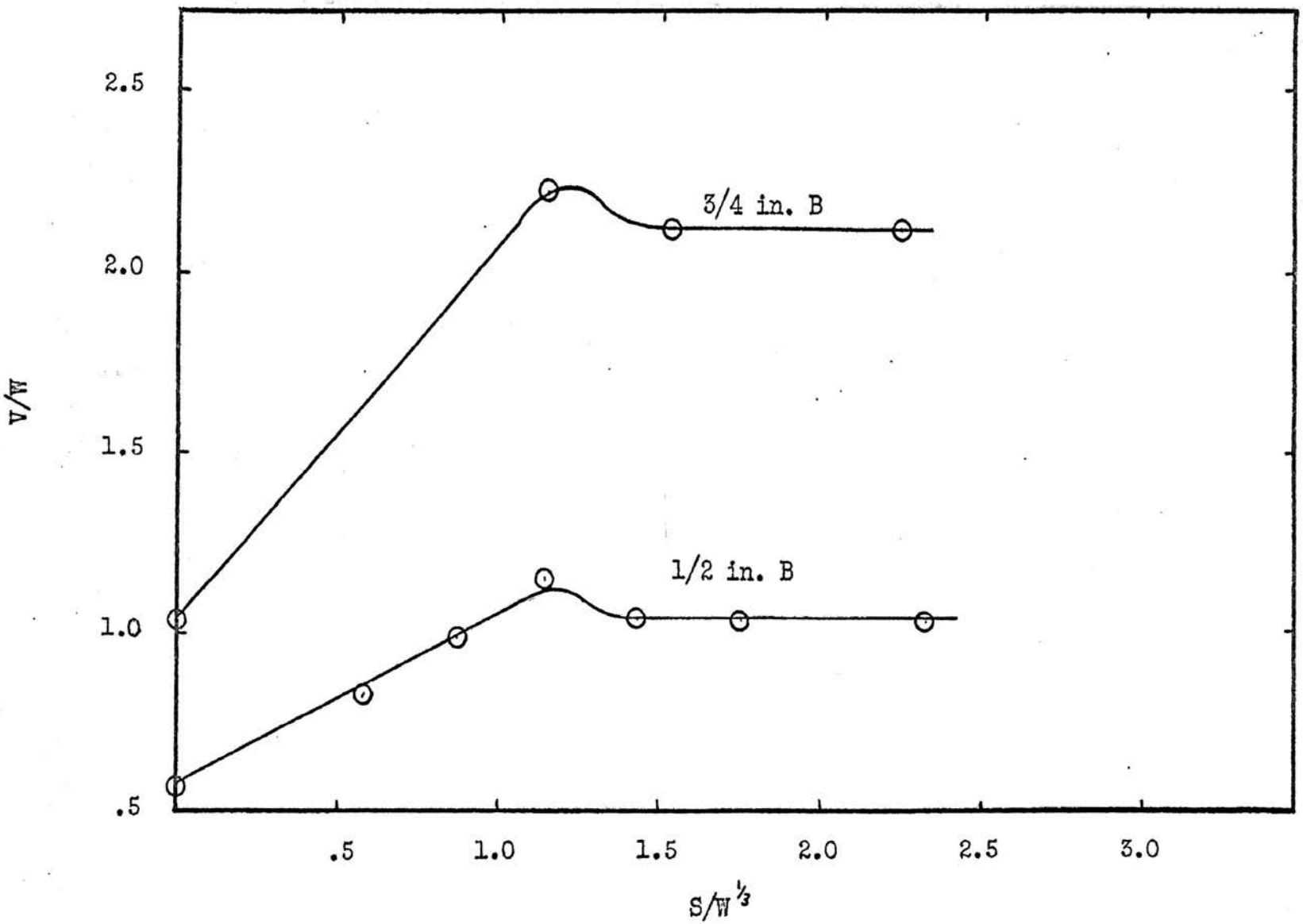

Figure 16. Crater Volume/Charge Weight vs. Explosive Spacing/(Charge Weight)$^{1/3}$ for Mortar (L/B = 6)

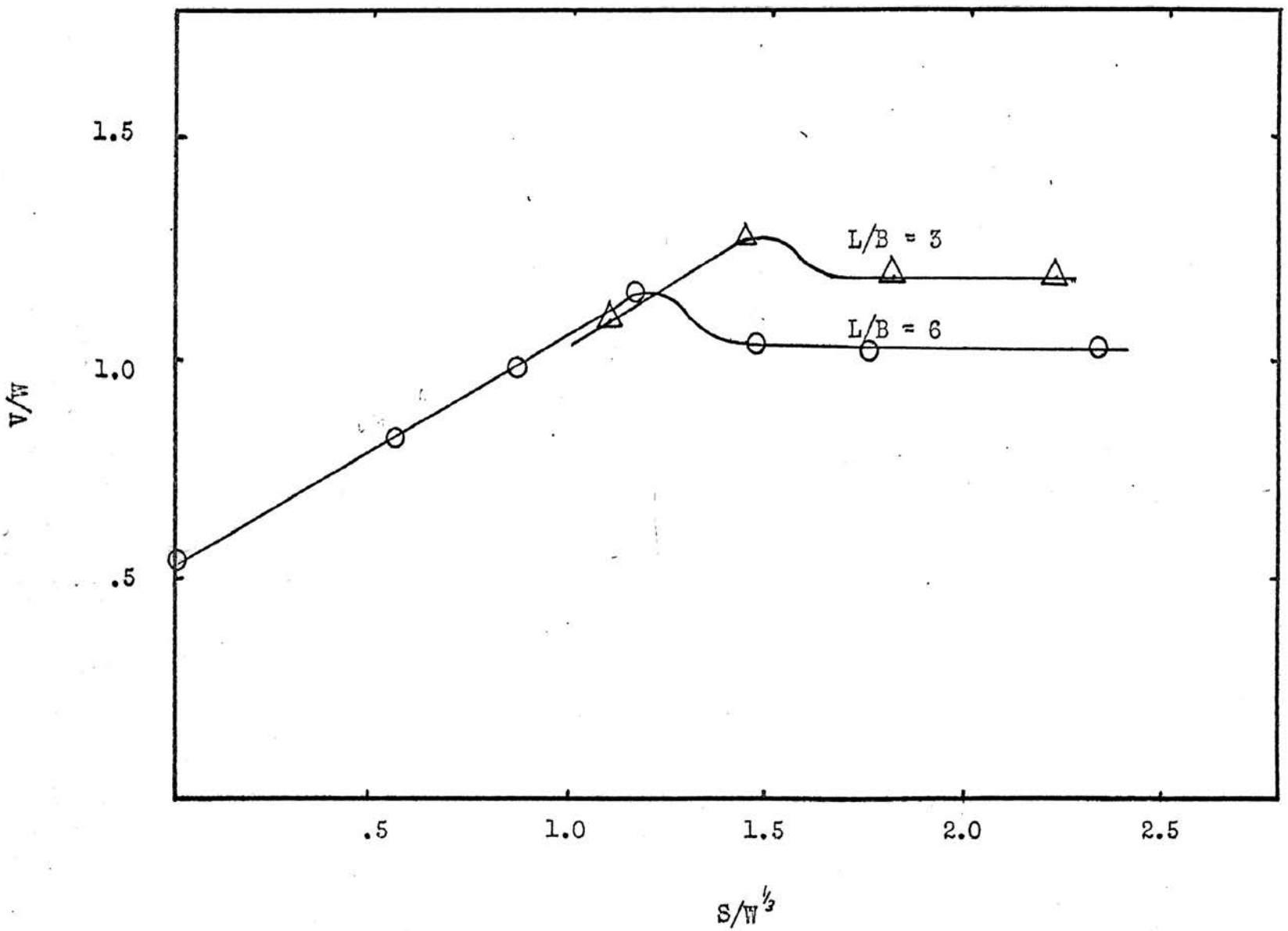

Figure 17. Crater Volume/Charge Weight vs. Explosive Spacing/(Charge Weight)$^{1/3}$ for Mortar (1/2 in. B)

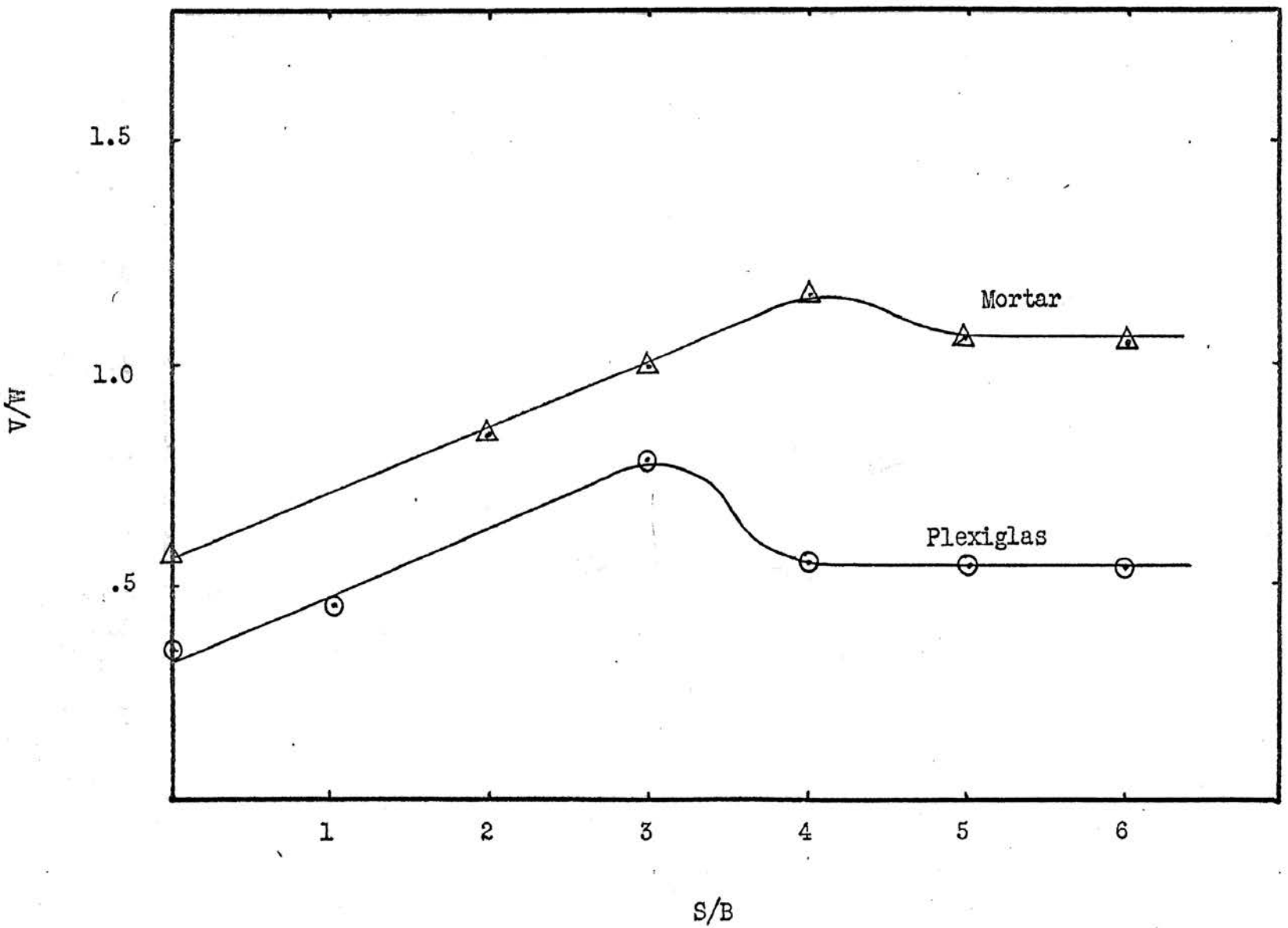

Figure 18. Crater Volume/Charge Weight vs. Explosive Spacing/Burden (L/B = 6, 1/2 in. B)

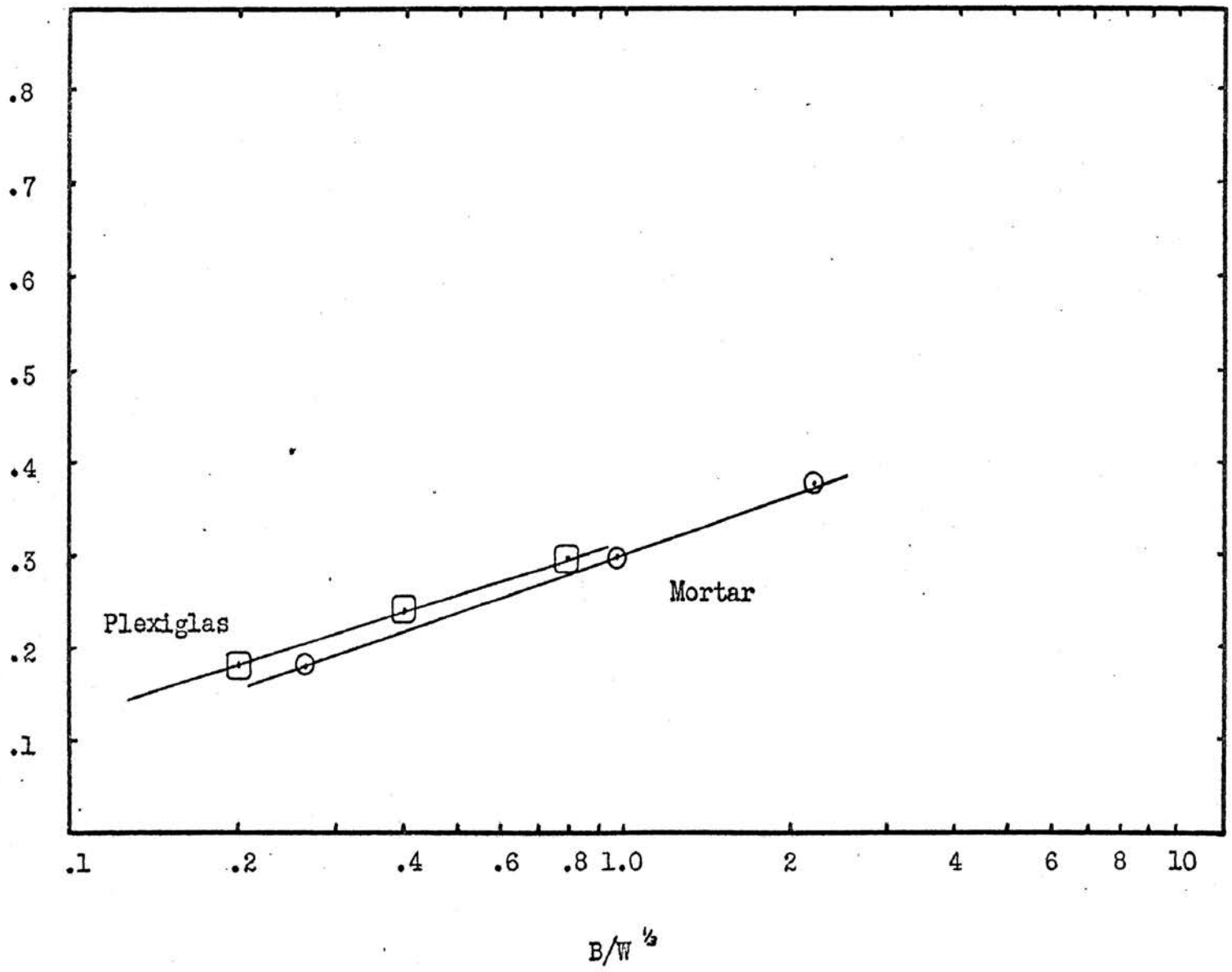

Figure 19. Crater Volume/Charge Weight vs. Burden/(Charge Weight)$^{1/3}$ (L/B = 6, S/B = 3).

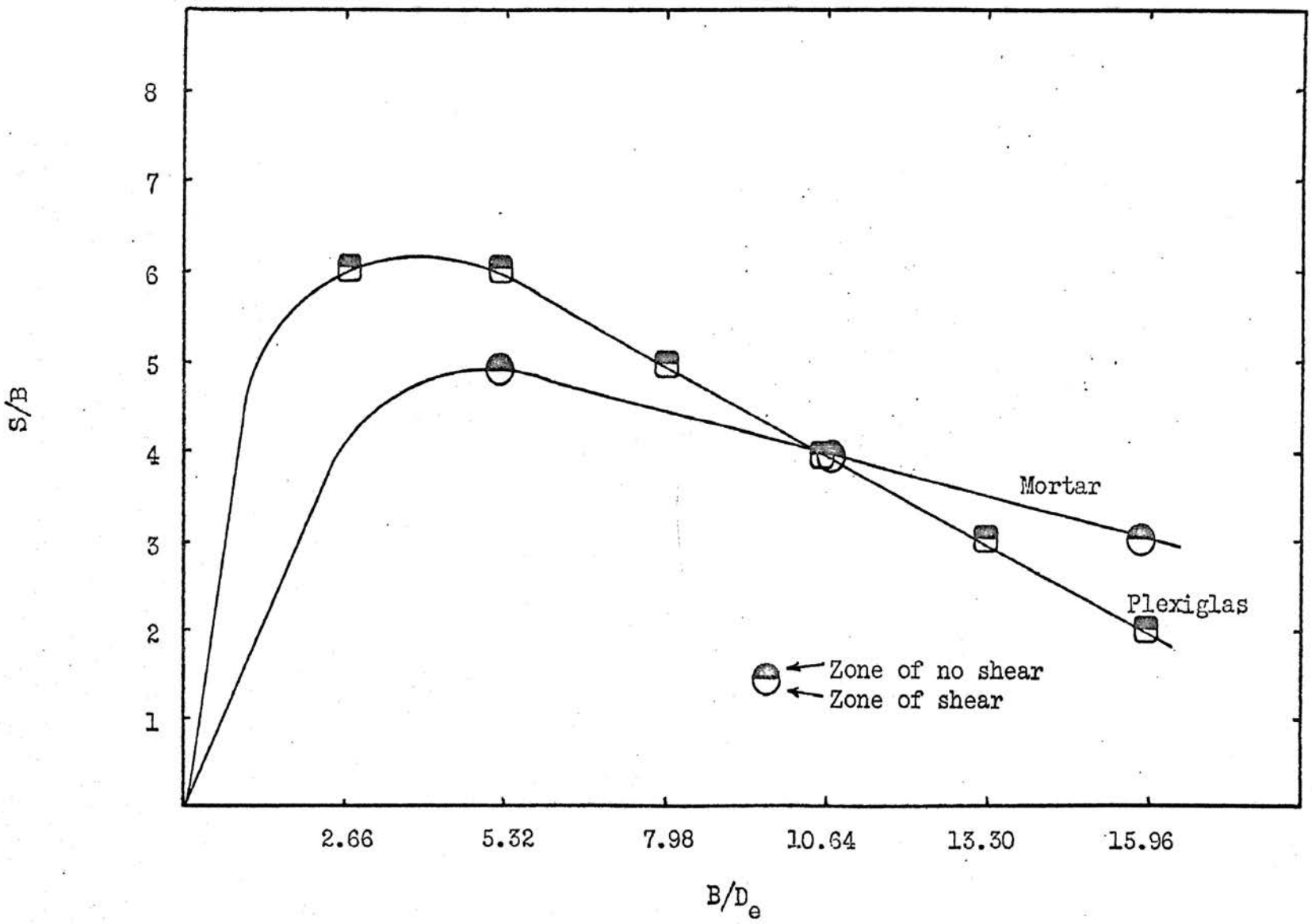

Figure 20. Charge Spacing/Burden vs. Burden/Charge Diameter (L/B = 6)

In Chapter II, it was noted that the characteristic burden for a material could be determined from firing single shots, and that the burden was not related to the spacing of simultaneously initiated charges. It has been observed in the models tested, that correct spacing caused interaction between charges and larger burdens could be placed on the materials. The characteristic burden for a single charge in Plexiglas was not increased by using twice the amount of explosive. The bottom of the charge was not broken out (Plate III and Plate IV) although the sample in Plate III had 20-grain MDF as the explosive, while the sample in Plate IV had only 10-grain MDF. The fracture pattern and the amount of material broken were the same in both the above mentioned cases. The samples shown in Plates V and VI were fired under similar conditions, the only difference was the spacing. When the interaction between charges was small, the holes functioned as independently fired charges, and the bottoms were not broken out (Plate V). At the correct spacing, the interaction caused the bottom to break out (Plate VI). The same phenomena could be seen in mortar and seemed independent of the L/B ratio (Plates VII, VIII, IX, X and XI). It was observed that the burden necessary to completely break the entire charge length for a single charge in Plexiglas and mortar was .375 and .50 inches, respectively. Using simultaneously initiated charges, burdens of .5 inches for Plexiglas and .75 inches for mortar could be used.

The influence of simultaneously initiated multiple charges on the fraction of the charge length broken is presented in Figure 21. The single charge never broke the material over the entire charge length (2). The properly spaced, simultaneously initiated, multiple charges

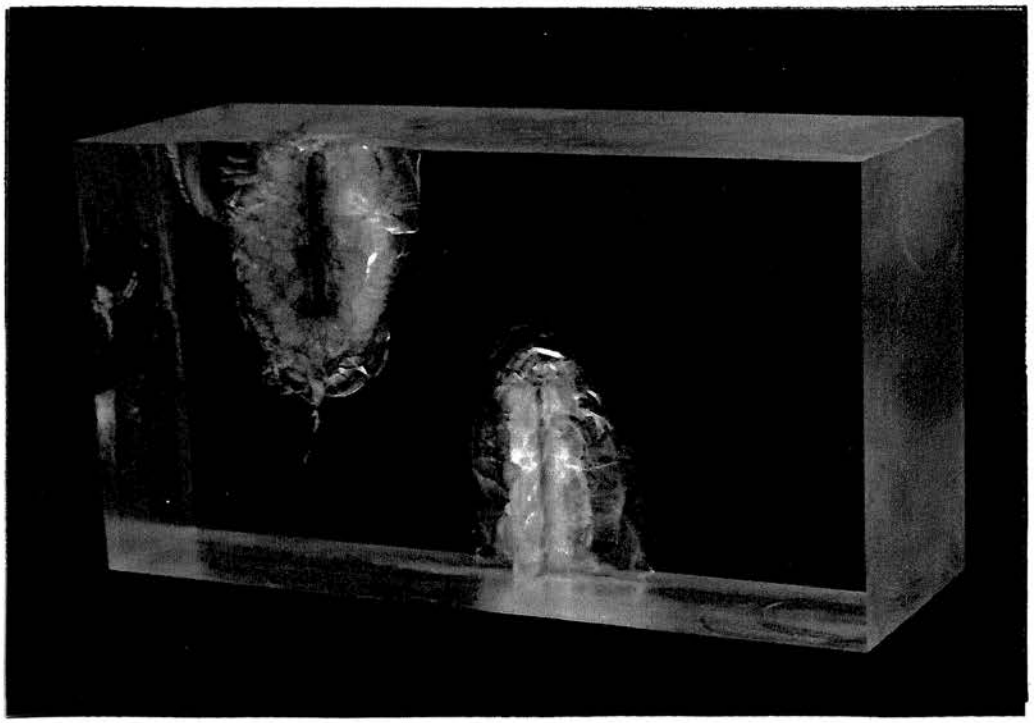

Plate III. MDF (20-grain) detonated in Plexiglas. (.5-inch Burden, Charge Length 3 inches)

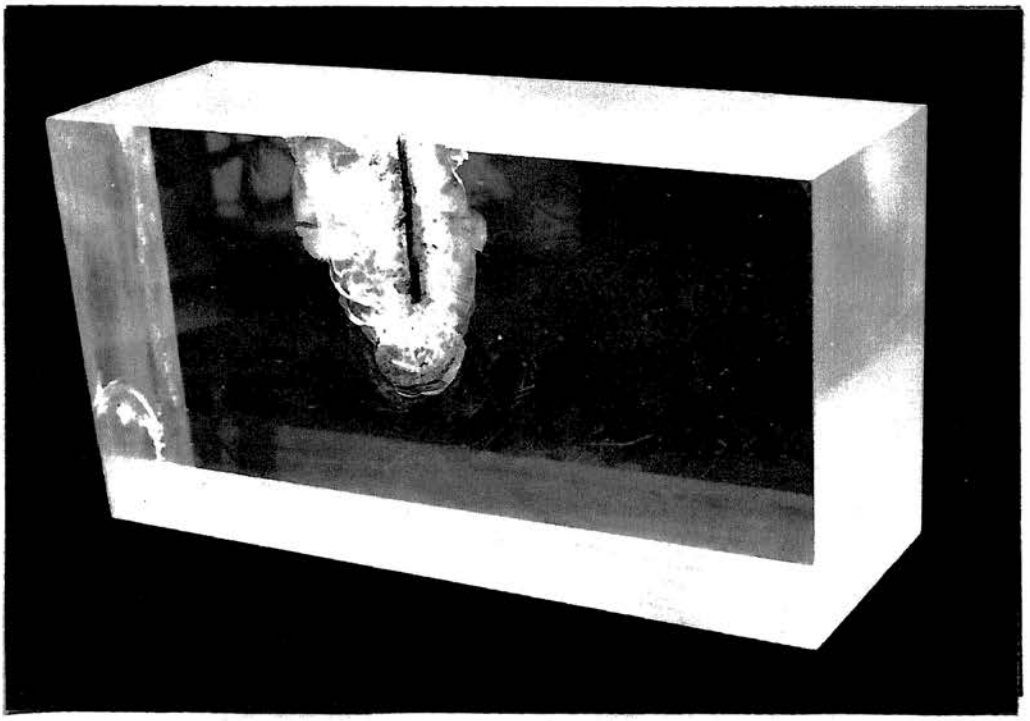

Plate IV. MDF (10-grain) detonated in Plexiglas. (.5-inch Burden, Charge Length 3 inches)

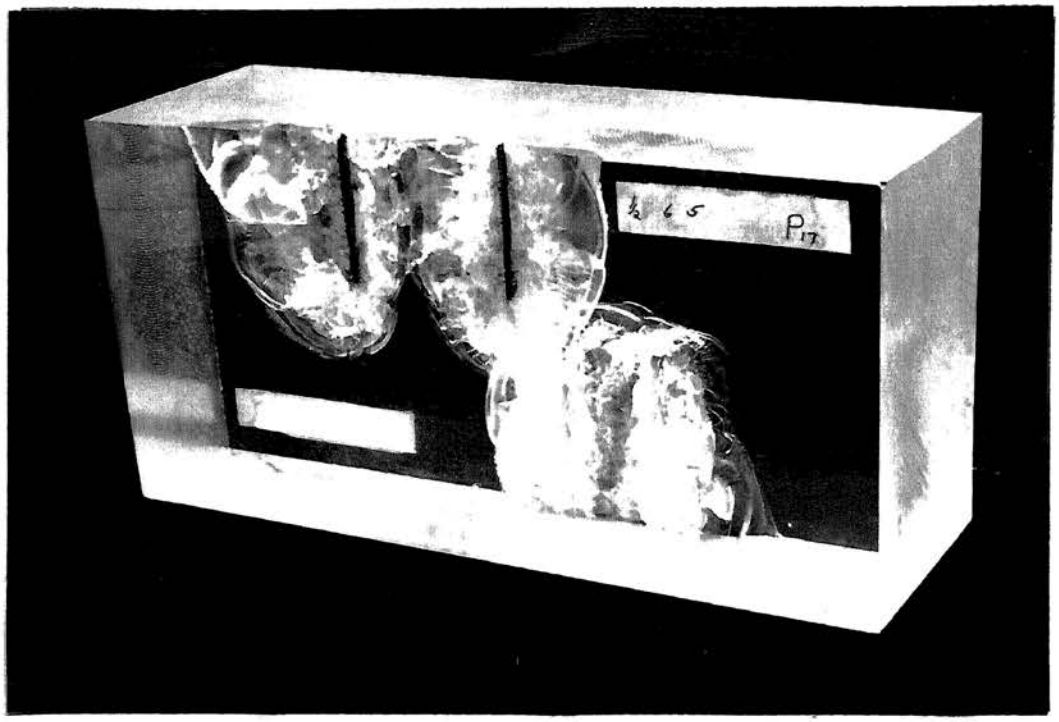

Plate V. MDF (10-grain) detonated in Plexiglas. (.5-inch Burden, Charge Length 3-inches, 2.5-inch spacing)

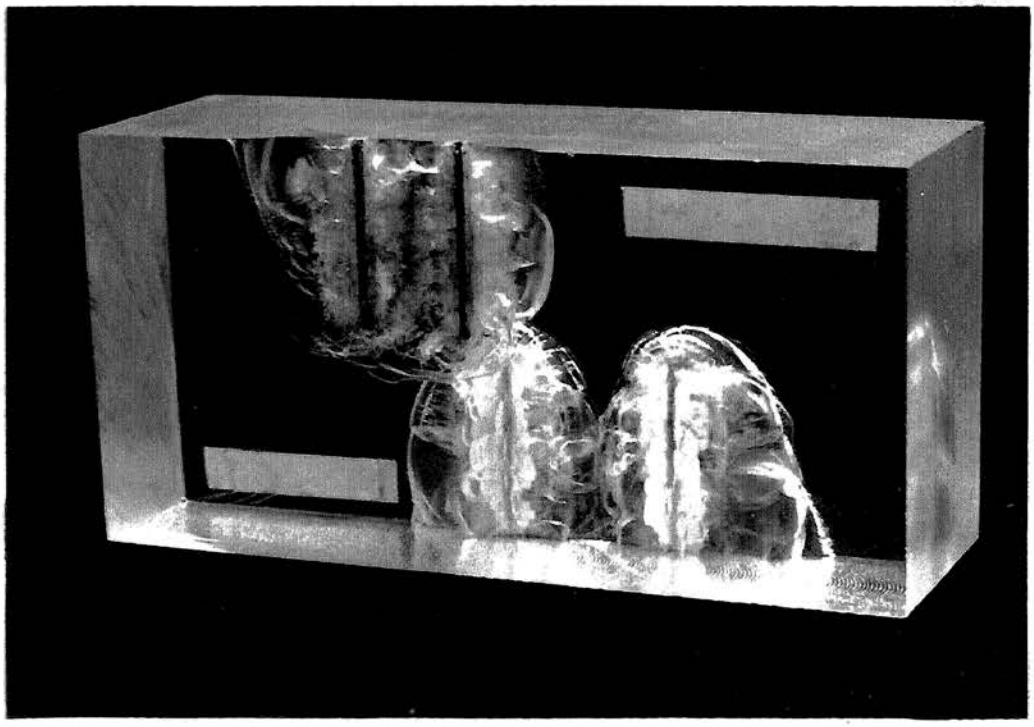

Plate VI. MDF (10-grain) detonated in Plexiglas. (.5-inch Burden, Charge Length 3-inches, 1.5-inch spacing)

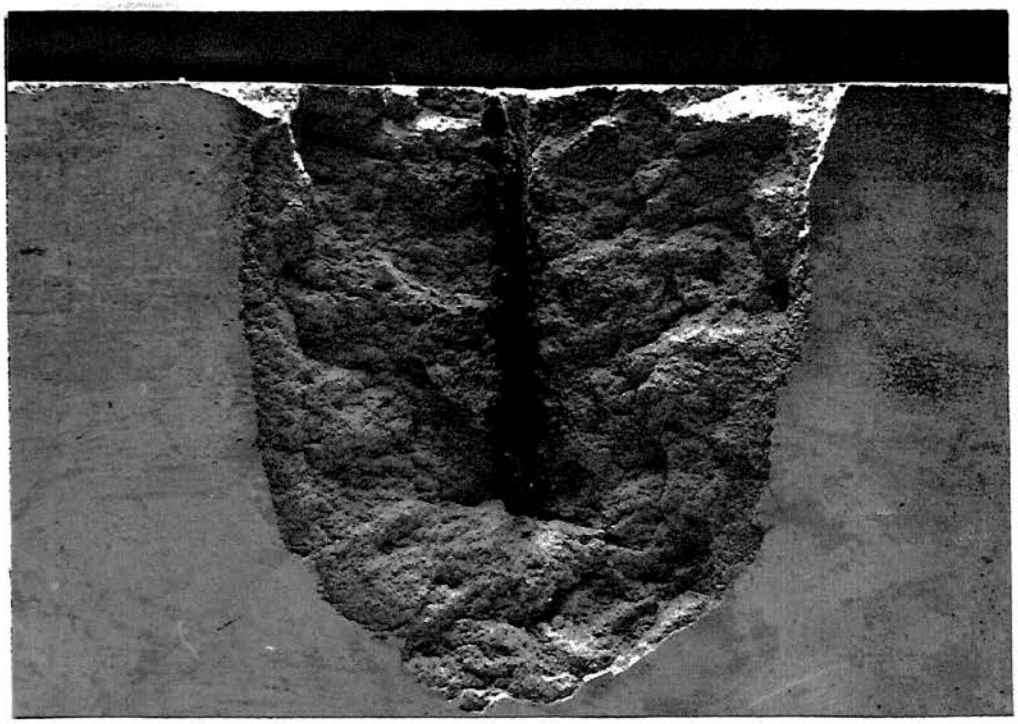

Plate VII. MDF (10-grain) detonated in Mortar. (.75-inch Burden, Charge Length 4.5-inches)

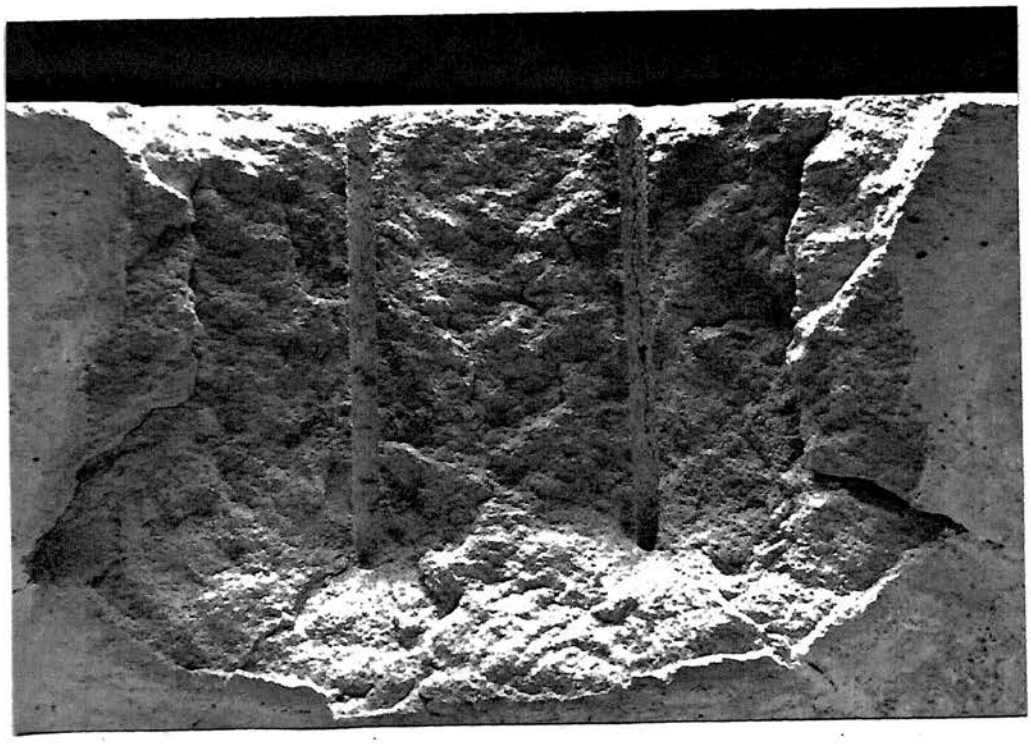

Plate VIII. MDF (10-grain) detonated in Mortar. (.75-inch Burden, Charge Length 4.5-inches, 2.25 inch spacing)

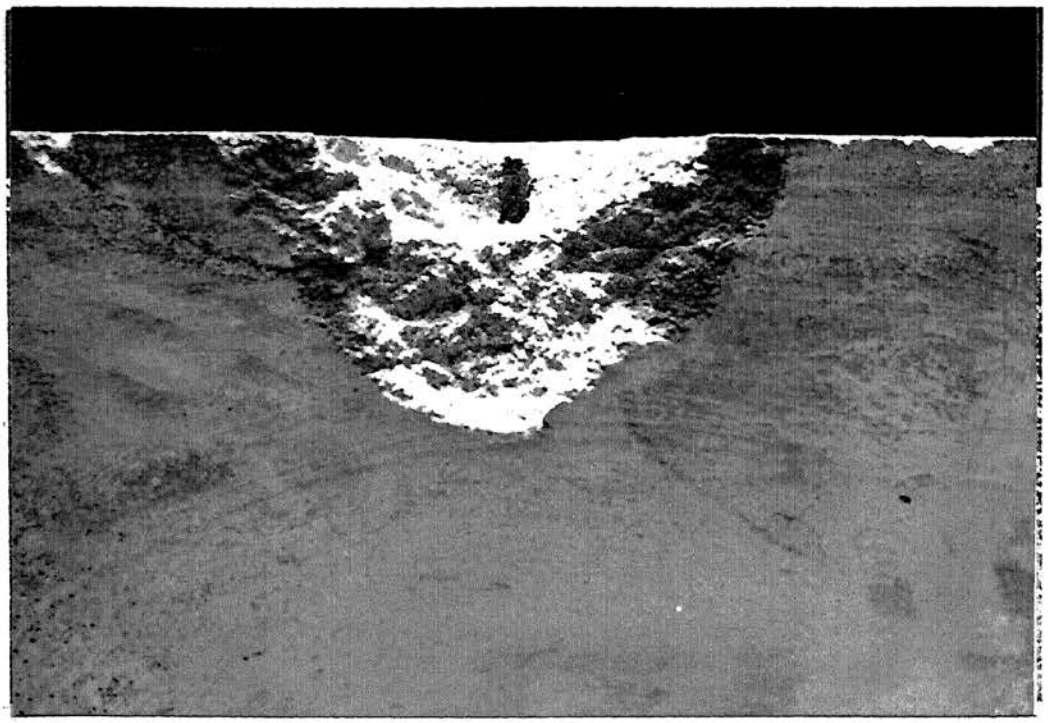

Plate IX. MDF (10-grain) detonated in Mortar. (.75-inch Burden, Charge Length 1.5-inches)

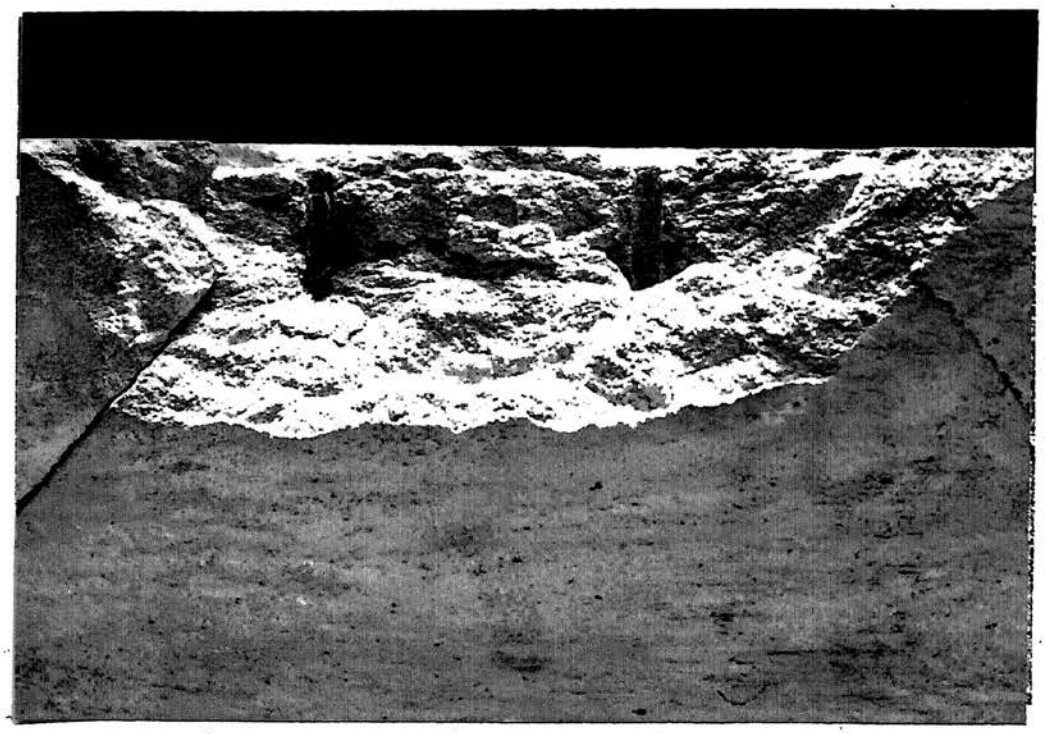

Plate X. MDF (10-grain) detonated in Mortar. (.75-inch Burden, Charge Length 1.5-inches, 2.25-inch spacing)

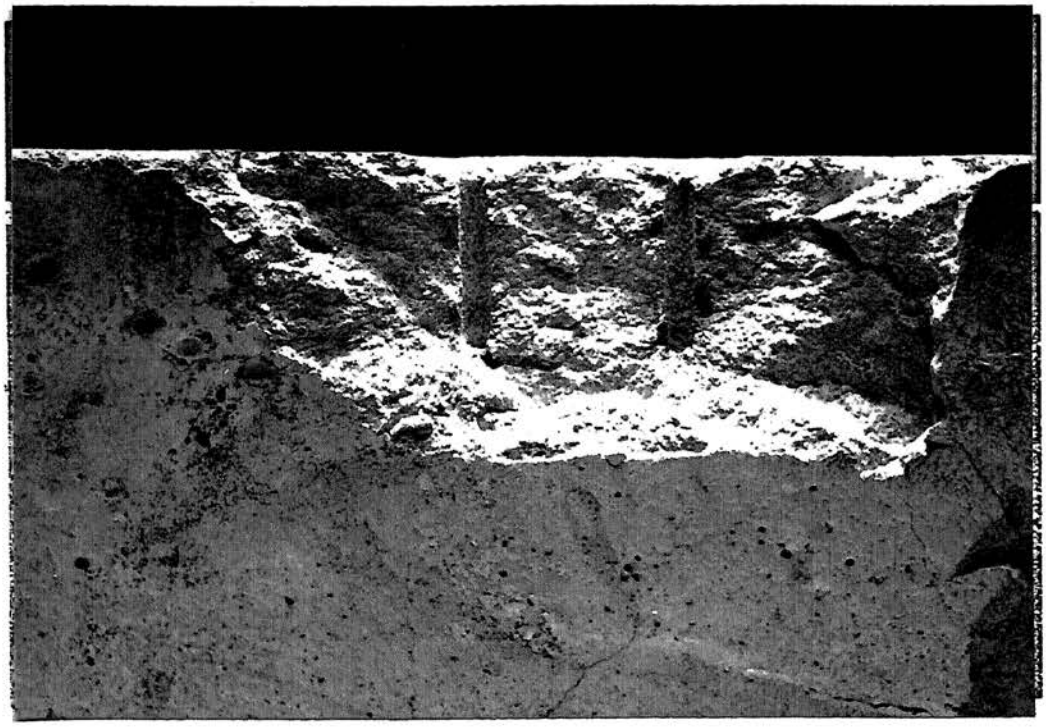

Plate XI. MDF (10-grain) detonated in Mortar. (.75-inch Burden, Charge Length 1.5-inches, 1.5-inch spacing)

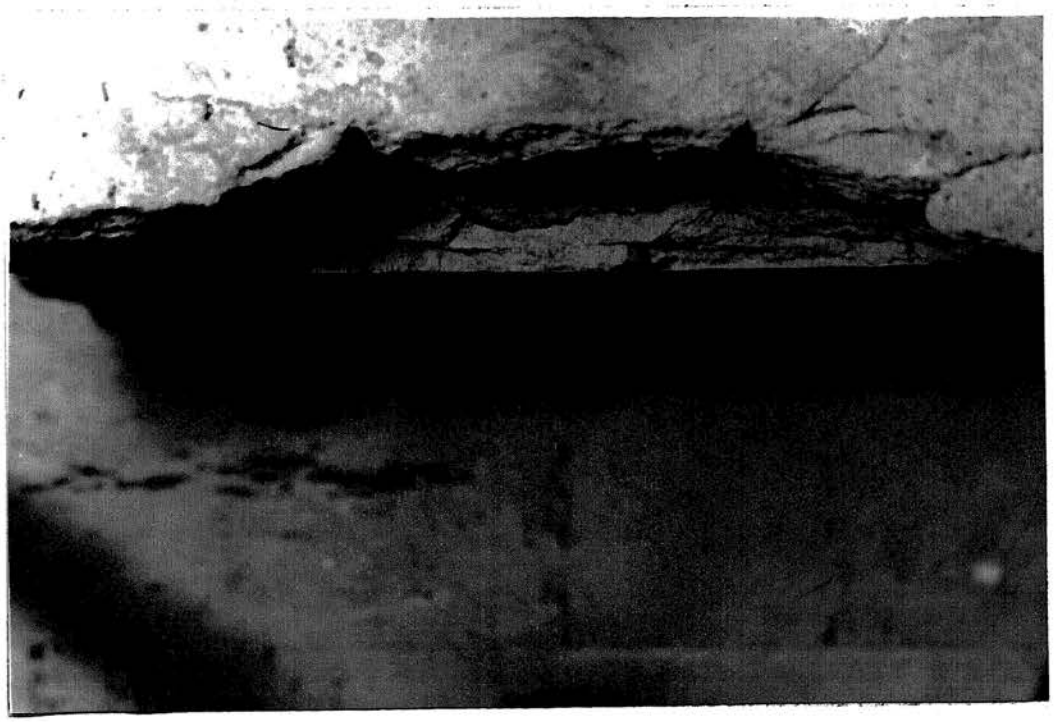

Plate XII. Plan View of Toe left when Burden was too large to completely break out

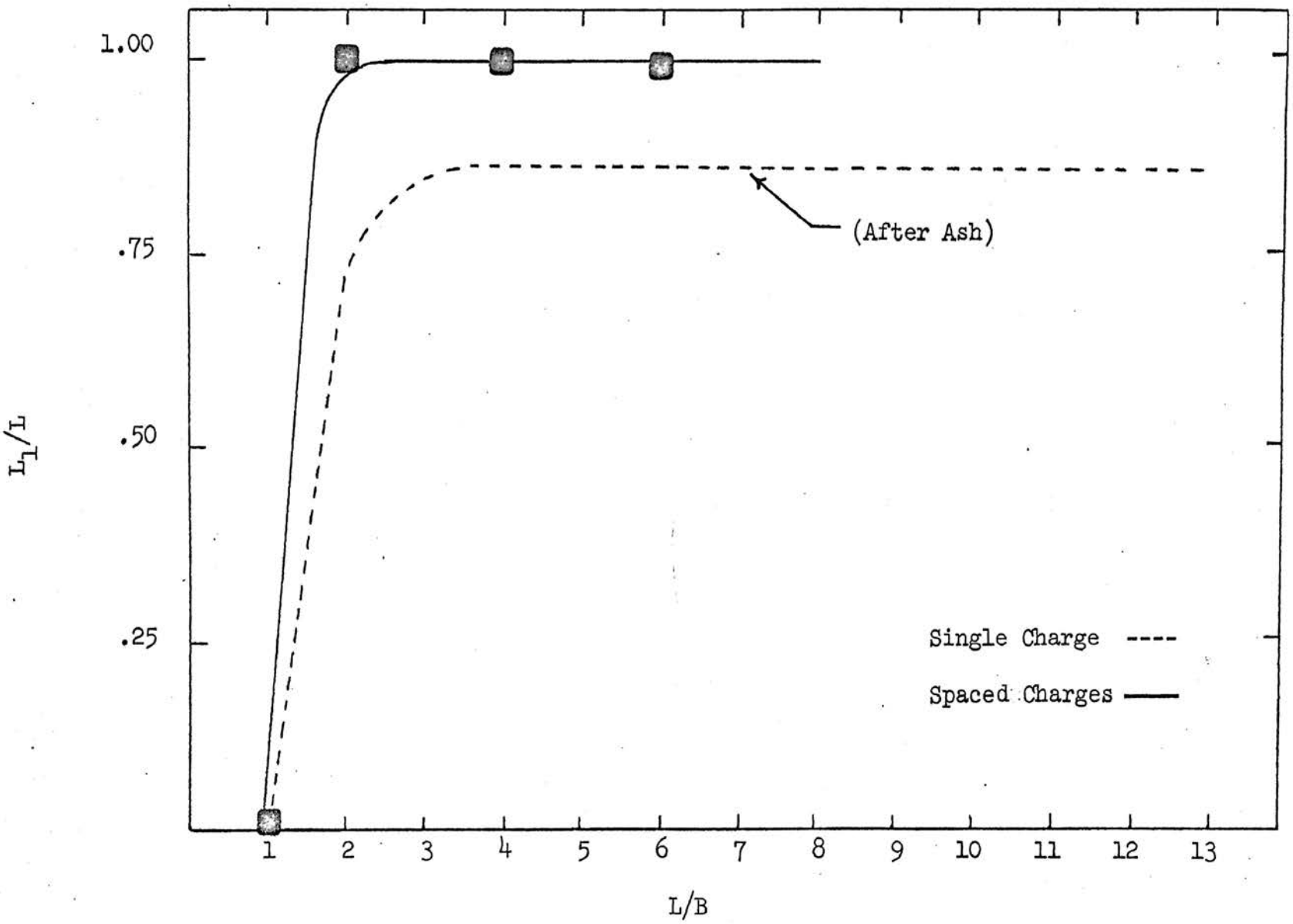

Figure 21. Charge Length Broken/Total Charge Length vs. Total Charge Length/Burden (Plexiglas, 1/2-inch Burden)

produced perfect craters with the same burden. Plate XII. shows the type of breakage in the toe of a mortar sample when the spacing was too great to completely break the material over the entire charge length.

V. CONCLUSIONS

The following conclusions are supported by the results from this investigation:

1. Charge length was important in the design of the spacing for low L/B ratio simultaneously initiated charges.
2. Noncoherent wave fronts were present in the collar region. A conical wave did not exist in this region, but was formed at some depth below the surface. This depth was dependent on the explosive and material's properties.
3. Scabbing due to the effects of the shock wave did not occur under normal model blasting conditions.
4. The optimum burden for single charges was not necessarily the optimum burden for multiple charges which were simultaneously initiated. Due to stress interactions, a larger burden could be used for simultaneously initiated charges.

VI. RECOMMENDATIONS FOR FURTHER STUDY

This investigation has suggested the following areas for further study:

1. A mathematical solution of the stress distribution in the collar, and its effect on spacing should be undertaken.

2. It would be interesting to study the formation of fractures in the collar and toe by means of high speed photography.

3. The effects of stemming length on the stress distribution in the collar region should be established.

4. A study should be made in regard to the effects of geologic structures on the spacing of explosive charges.

5. The characteristic stress mechanics involved at the toe of open and closed bottom benches should be investigated.

6. The role of the material's properties in regard to spacing of simultaneously initiated charges should be defined.

APPENDIX I.

LIST OF ABBREVIATIONS AND SYMBOLS

B	Burden dimension (in.)
D_e	Diameter of explosive (in.)
D_b	Diameter of borehole (in.)
E	Modulus of elasticity (psi)
L_l	Charge length broken by explosive
L	Total charge length (in.)
S	Spacing (in.)
Sge	Specific gravity of explosive
Sgr	Specific gravity of rock
V	Crater volume $(in.)^3$
V_e	Detonation velocity of explosive (fps)
V_p	Longitudinal wave velocity (fps)
V_s	Shear wave velocity (fps)
W	Weight of explosive charge (grains)
x	Crater angle in plane of charge diameter (deg.)
y	Crater angle in plane of charge length (deg.)
Z	Acoustical impedance $(lb\text{-}sec/ft^3)$
α	Angle of incidence of a compressive pulse at an impedance discontinuity
μ	Poisson's ratio
σ_c	Compressive strength of specimen (psi)
σ_t	Tensile strength of specimen (psi)
τ	Shear strength of specimen (psi)
ϕ	Angle of internal friction

APPENDIX II.

DERIVATION OF SIMILITUDE RATIOS

General Equation

$$(1)\quad S = f\,(V_p\ B\ L\ E\ V_e\ D_e\ \gamma\ \sigma_t\ \phi\ \alpha\ Sgr\ Sge\ \mu)$$

Equation (1) may be written as

$$(2)\quad C\ S^{C_1} V_p^{C_2} B^{C_3} L^{C_4} E^{C_5} V_e^{C_6} D_e^{C_7} \gamma^{C_8} \sigma_t^{C_9} \phi^{C_{10}} \alpha^{C_{11}} Sgr^{C_{12}} Sge^{C_{13}} \mu^{C_{14}} = 1$$

The corresponding dimensional equation in units of Force (F), Length (L) and Time (T) is

$$(3)\quad 0 = (L)^{C_1} (LT^{-1})^{C_2} (L)^{C_3} (L)^{C_4} (FL^{-2})^{C_5} (LT^{-1})^{C_6} (L)^{C_7} (FL^{-2})^{C_8} (FL^{-2})^{C_9}$$

From which three auxiliary equations may be written

$$(4)\quad F:\ C_5 + C_8 + C_9 = 0$$

$$(5)\quad L:\ C_1 + C_2 + C_3 + C_4 - 2C_5 + C_6 + C_7 - 2C_8 - 2C_9 = 0$$

$$(6)\quad T:\ -C_2 - C_6 = 0$$

Since three equations are available for solving for nine unknowns, arbitrary values are assigned to six unknowns. Many combinations are possible: of these the one involving C_1, C_2, C_4, C_7, C_8 and C_9 was chosen for illustration. The determinant of the coefficients of the remaining terms (C_3, C_5 and C_6) is

$$\begin{vmatrix} 0 & 1 & 0 \\ 1 & -2 & 1 \\ 0 & 0 & -1 \end{vmatrix} = 1$$

Since this is not equal to zero, the resulting equations are independent and valid.

APPENDIX II.

(continued)

Arbitrary values are assigned as follows:

$$C_1 = 1$$

$$C_2, C_4, C_7, C_8, C_9 = 0$$

These values are substituted into Equation (4), (5) and (6).

$$C_5 = 0$$

$$1 + C_3 - 2C_5 + C_6 = 0$$

$$- C_6 = 0$$

So $C_3 = -1 \quad C_5 = 0 \quad C_6 = 0$

From this and Equation (2) dropping C

$$\pi_1 = \frac{S}{B}$$

which is dimensionless

Other terms may be found by selecting different combinations of arbitrary values for the exponents. By letting C_2, C_4, C_7, C_8 and C_9 in turn equal unity, with the other exponents equal to zero, we get

$$\pi_2 = V_p/V_e$$

$$\pi_3 = L/B$$

$$\pi_4 = \frac{D_e}{B}$$

$$\pi_5 = \gamma/E$$

$$\pi_6 = \sigma_t/E$$

APPENDIX II.

(continued)

By adding the dimensionless quantities from Equation (2), five more terms result:

$$\pi_7 = \phi$$

$$\pi_8 = \alpha$$

$$\pi_9 = \text{Sgr}$$

$$\pi_{10} = \text{Sge}$$

$$\pi_{11} = \mu$$

A general solution may be written as

$$\frac{S}{B} = f\left(\frac{V_p}{V_e}, \frac{L}{B}, \frac{D_e}{B}, \frac{\tau}{E}, \frac{\sigma_t}{E}, \phi, \alpha, \text{Sgr}, \text{Sge}, \mu\right)$$

APPENDIX III.

SONIC VELOCITIES

A. Longitudinal

Material	Distance (in.)	Time (u sec)	Velocity (fps)
Plexiglas	4.315	41	8,760
Plexiglas	4.250	40	8,850
Plexiglas	4.070	39	8,680
Mortar	11.400	73	13,014
Mortar	12.000	78	12,903
Mortar	12.000	78	12,903
Mortar	10.570	67	13,037
Mortar	12.000	77	13,000
Mortar	11.625	74	13,100
Dolomite	3.125	18	14,460
Dolomite	8.312	46	14,730

Plexiglas	Mean Value	8,764
Mortar	Mean Value	13,000
Dolomite	Mean Value	14,596

APPENDIX III.

(continued)

B. Transverse

Material	Distance (in.)	Time (μ sec)	Velocity (fps)
Plexiglas	1.468	35	3,497
Granite	1.562	14	9,285
Hydrostone	1.750	22	6,627
Mortar	1.219	12	8,450
Mortar	2.344	24	8,120
Mortar	3.031	29	8,700
Mortar	4.063	41	8,250
Dolomite	1.625	16	8,450
Dolomite	2.219	21	8,790

Mortar	Mean Value	8,390
Dolomite	Mean Value	8,620

APPENDIX IV.

COMPRESSIVE STRENGTH OF MORTAR

Sample	Loading Rate (Lbs/sec)	Diameter (in.)	Length (in.)	Area ($in.^2$)	Load at Failure (psi)	Stress (psi)
A_1	100	2.125	4.532	3.548	25,450	7,173
A_2	100	2.125	4.625	3.548	24,950	7,032
A_3	100	2.125	4.438	3.548	25,540	7,198
B_1	100	2.125	4.469	3.548	25,500	7,187
B_2	100	2.125	4.500	3.548	25,500	7,187
B_3	100	2.125	4.469	3.548	25,200	7,102

Mean Value Sample A 7122
Mean Value Sample B 7148
Mean Value Sample A and B 7140

APPENDIX V.

TENSILE STRENGTH OF MORTAR

Sample	Loading Rate (lbs/sec)	Length (in.)	Diameter (in.)	Load at Failure (psi)	Stress (psi)
A_1	100	2.562	2.125	3246	379.72
A_2	100	2.562	2.125	3061	358.07
A_3	100	2.094	2.125	2440	360.14
A_4	100	2.406	2.125	2834	353.15
B_1	100	2.500	2.125	3029	363.20
B_2	100	2.500	2.125	3520	372.20
B_3	100	2.375	2.125	3051	384.90
B_4	100	2.219	2.125	2650	357.77

Mean Value	Sample A	362.77
Mean Value	Sample B	369.52
Mean Value	Sample A and B	366.15

APPENDIX VI.

SPECIFIC GRAVITY MEASUREMENTS

A. Mortar

Sample	Weight (Lb)	Volume (ft^3)	S.G.
A_1	62.8	.4612	2.18
A_2	61.6	.4384	2.25
A_3	133.8	.9792	2.19
A_4	135.7	.9875	2.20
B_1	58.6	.4229	2.22
B_2	61.0	.4524	2.16
B_3	134.2	.9735	2.21
B_4	134.9	.9875	2.19

Mean Value	Sample A	2.205
Mean Value	Sample B	2.195
Mean Value	Samples A and B	2.200

APPENDIX VII.

DERIVATION OF CRATER VOLUME EQUATION

A. Case 1 (Fig. 22)

Volume of Section A

$$V_A = LB \left(\frac{B}{\tan x} + \frac{D_b}{2}\right)$$

Volume of Section B assuming Section B is one quarter of an ellipsoid whose volume is $\frac{\pi}{3}$ abc where

$$a = \frac{B}{\tan x} + \frac{D_b}{2}$$

$$b = \frac{B}{\tan y}$$

$$c = B$$

$$V_B = \frac{\pi}{3} \left(\frac{B}{\tan x} + \frac{D_b}{2}\right) \left(\frac{B}{\tan y}\right) (B)$$

$$V_B = \frac{\pi B^2}{3 \tan y} \left(\frac{B}{\tan x} + \frac{D_b}{2}\right)$$

Total volume in Case 1 for one horizontal crater is

$V_T = V_A + V_B$ (Figure 23)

$$V_T = LB \left(\frac{B}{\tan x} + \frac{D_b}{2}\right) + \frac{\pi B^2}{3 \tan y} \left(\frac{B}{\tan x} + \frac{D_b}{2}\right)$$

Volume of two horizontal craters

$$V_T = 2B \left(\frac{B}{\tan x} + \frac{D_b}{2}\right) \left(L + \frac{\pi B}{3 \tan y}\right)$$

B. Case 2 (Fig. 22)

Volume of Section C

$$V_C = LB \left(S + D_b + \frac{B}{\tan x}\right)$$

APPENDIX VII.

(continued)

Volume of Section D assuming D is again one quarter of an ellipsoid

$$a = 1/2 \left(S + \frac{2B}{\tan x} + D_b\right)$$

$$b = \frac{B}{\tan y}$$

$$c = B$$

$$V_D = \frac{\pi}{3} \left(\frac{S}{2} + \frac{B}{\tan x} + \frac{D_b}{2}\right) \left(\frac{B}{\tan y}\right) (B)$$

$$V_D = \frac{\pi B^2}{3 \tan y} \left(\frac{S}{2} + \frac{B}{\tan x} + \frac{D_b}{2}\right)$$

Total volume for Case 2 (Fig. 23)

$$V_T = LB \left(S + \frac{B}{\tan x} + D_b\right) + \frac{\pi B^2}{3 \tan y} \left(\frac{S}{2} + \frac{B}{\tan x} + \frac{D_b}{2}\right)$$

APPENDIX VII

(continued)

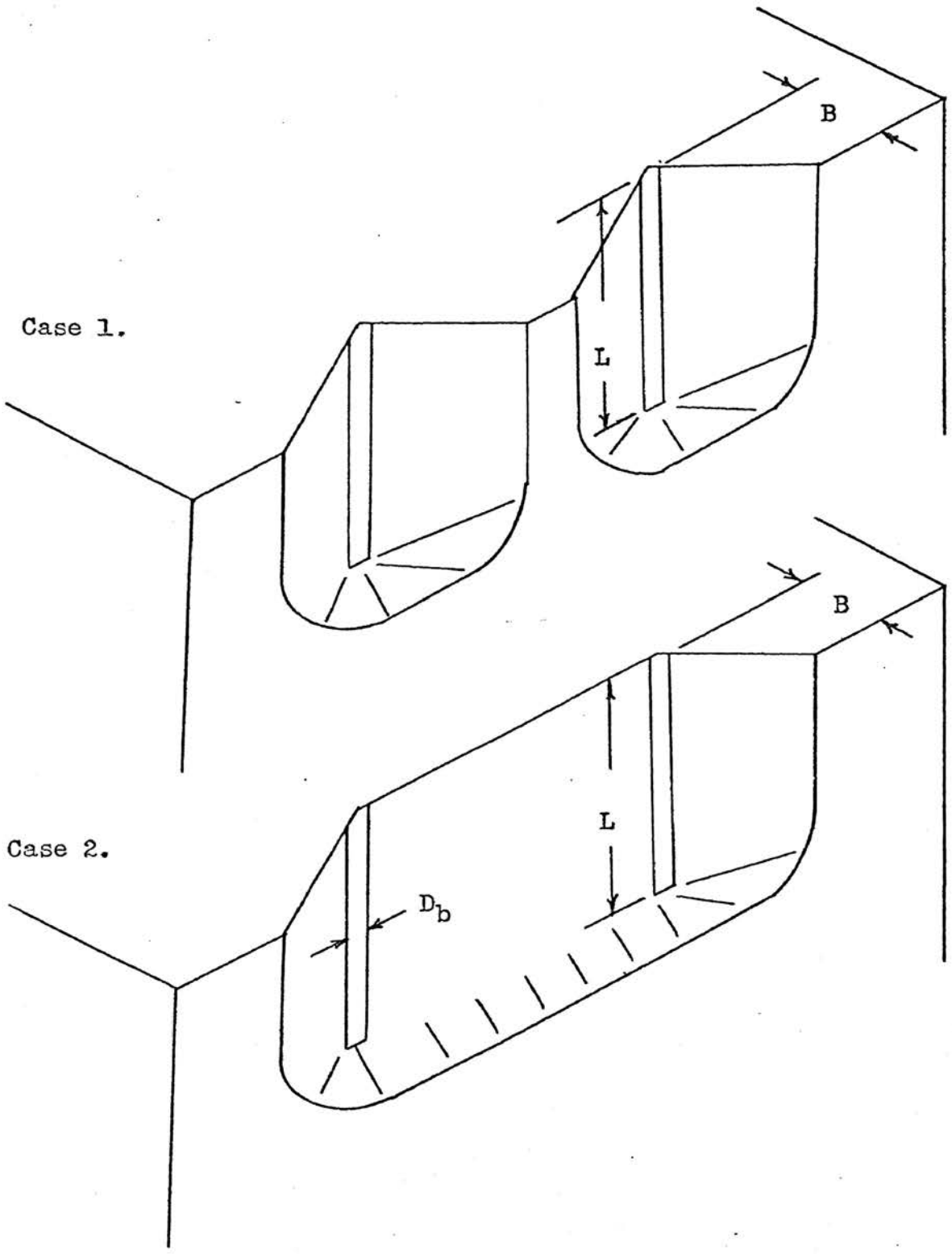

Figure 22. Dimension of Crater Forms

APPENDIX VII

(continued)

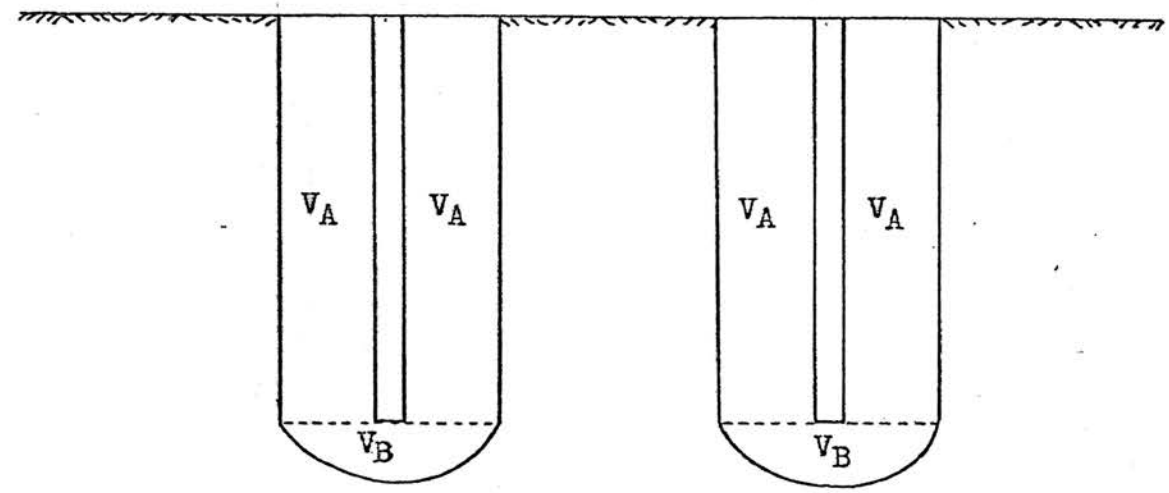

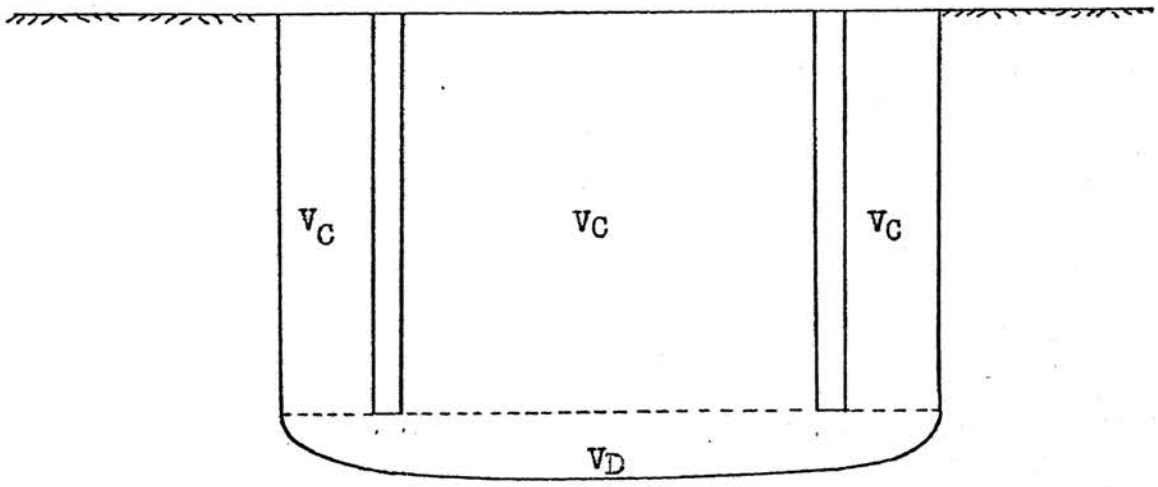

Figure 23. Volumes of Crater Forms

APPENDIX VIII.

EXPERIMENTAL DATA FOR SPACED CHARGES

A. Plexiglas

Burden (in.)	Length (in.)	Spacing (in.)	L/B	S/B	L_1/L	Angle x (deg.)	Angle y (deg.)	Crater Form
.25	0.0	0.0	0.0	0.0	---	---	---	---
.25	0.0	0.25	0.0	1.0	---	---	---	---
.25	0.125	0.0	0.5	0.0	1.0	32	26	1
.25	0.125	0.25	0.5	1.0	1.0	34	30	2
.25	0.125	0.5	0.5	2.0	1.0	32	35	2
.25	0.125	0.75	0.5	3.0	1.0	30	45	1
.25	0.25	0.5	1.0	2.0	1.0	39	32	2
.25	0.25	0.75	1.0	3.0	1.0	30	30	2
.25	0.25	1.0	1.0	4.0	1.0	35	35	1
.25	0.5	0.5	2.0	2.0	1.0	35	35	1
.25	0.5	0.75	2.0	3.0	1.0	32	45	2
.25	0.5	1.0	2.0	4.0	1.0	40	40	1
.25	1.0	0.75	4.0	3.0	1.0	30	45	2
.25	1.0	1.25	4.0	5.0	1.0	30	32	1

APPENDIX VIII.

(continued)

Burden (in.)	Length (in.)	Spacing (in.)	L/B	S/B	L_1/L	Angle x (deg.)	Angle y (deg.)	Crater Form
.25	1.5	0.0	6.0	0.0	1.0	30	40	1
.25	1.5	0.25	6.0	1.0	1.0	32	38	2
.25	1.5	0.75	6.0	3.0	1.0	30	25	2
.25	1.5	1.25	6.0	5.0	1.0	30	30	2
.25	1.5	1.5	6.0	6.0	1.0	30	35	1
.25	3.0	1.5	12.0	6.0	1.0	30	35	1
.25	3.5	1.25	14.0	5.0	1.0	30	30	2
.375	0.188	0.0	0.5	0.0	---	---	---	---
.375	0.375	0.0	1.0	0.0	0.5	32	32	1
.375	1.125	1.5	3.0	4.0	1.0	30	45	1
.375	1.875	1.125	5.0	3.0	1.0	35	30	2
.375	2.25	1.5	6.0	4.0	1.0	30	35	2
.375	2.25	1.875	6.0	5.0	1.0	30	30	1
.375	3.375	1.5	9.0	4.0	1.0	30	45	2

APPENDIX VIII.

(continued)

Burden (in.)	Length (in.)	Spacing (in.)	L/B	S/B	L_1/L	Angle x (deg.)	Angle y (deg.)	Crater Form
.375	4.125	1.5	11.0	4.0	1.0	32	30	2
.375	4.5	1.875	12.0	5.0	1.0	30	45	1
.5	0.125	0.0	0.25	0.0	---	---	---	---
.5	0.25	0.0	0.5	0.0	---	---	---	---
.5	0.25	0.5	0.5	1.0	---	---	---	---
.5	0.5	0.0	1.0	0.0	---	---	---	---
.5	0.5	0.5	1.0	1.0	---	---	---	---
.5	0.75	0.0	1.5	0.0	0.66	36	40	1
.5	1.0	1.0	2.0	2.0	1.0	30	45	2
.5	2.0	1.0	4.0	2.0	1.0	39	45	2
.5	3.0	0.0	6.0	0.0	0.90	39	45	1
.5	3.0	0.5	6.0	1.0	1.0	30	43	2
.5	3.0	1.5	6.0	3.0	1.0	35	38	2
.5	3.0	2.0	6.0	4.0	0.79	30	30	1

APPENDIX VIII.

(continued)

Burden (in.)	Length (in.)	Spacing (in.)	L/B	S/B	L_1/L	Angle x (deg.)	Angle y (deg.)	Crater Form
.5	3.0	2.5	6.0	5.0	0.81	30	40	1
.5	4.5	2.0	9.0	4.0	0.80	30	42	1
.125	0.75	0.75	6.0	6.0	1.0	30	32	1
.625	3.75	1.25	6.0	2.0	1.0	31	45	2
.75	4.5	1.5	6.0	2.0	1.0	33	42	1

APPENDIX VIII.

(continued)

B. Mortar

Burden (in.)	Length (in.)	Spacing (in.)	L/B	S/B	L_1/L	Angle x (deg.)	Angle y (deg.)	Crater Form
.25	1.5	0.75	6.0	3.0	1.0	20	32	2
.25	1.5	1.25	6.0	5.0	1.0	20	31	2
.25	1.5	1.5	6.0	6.0	1.0	22	33	2
.375	2.25	0.0	6.0	0.0	1.0	19	30	1
.5	0.125	0.0	0.25	0.0	---	---	---	---
.5	0.25	0.0	0.5	0.0	1.0	22	32	1
.5	0.25	1.0	0.5	2.0	---	---	---	---
.5	0.5	1.0	1.0	2.0	1.0	21	33	2
.5	0.5	1.5	1.0	3.0	1.0	20	38	1
.5	1.0	1.0	2.0	2.0	1.0	22	33	2
.5	1.5	1.5	3.0	3.0	1.0	19	36	2
.5	1.5	2.0	3.0	4.0	1.0	22	30	2
.5	1.5	2.5	3.0	5.0	1.0	21	33	1

APPENDIX VIII.

(continued)

Burden (in.)	Length (in.)	Spacing (in.)	L/B	S/B	L_1/L	Angle x (deg.)	Angle y (deg.)	Crater Form
.5	3.0	0.0	6.0	0.0	1.0	20	32	1
.5	3.0	0.5	6.0	1.0	1.0	20	32	2
.5	3.0	1.0	6.0	2.0	1.0	20	31	2
.5	3.0	1.5	6.0	3.0	1.0	22	34	2
.5	3.0	2.0	6.0	4.0	1.0	19	33	2
.5	3.0	2.5	6.0	5.0	1.0	20	32	1
.5	3.0	3.0	6.0	6.0	1.0	20	32	1
.5	4.5	2.5	9.0	5.0	1.0	20	32	1
.75	0.375	0.0	0.5	0.0	---	---	---	---
.75	0.75	0.0	1.0	0.0	1.0	20	33	1
.75	1.5	1.5	2.0	2.0	1.0	20	37	2
.75	1.5	2.25	2.0	3.0	0.83	20	30	2
.75	2.25	2.25	3.0	3.0	1.0	19	34	2
.75	3.0	3.0	4.0	4.0	0.92	20	32	2

APPENDIX VIII.

(continued)

Burden (in.)	Length (in.)	Spacing (in.)	L/B	S/B	L_1/L	Angle x (deg.)	Angle y (deg.)	Crater Form
.75	4.5	0.0	6.0	0.0	0.88	20	30	1
.75	4.5	2.25	6.0	3.0	1.0	20	30	2
.75	4.5	3.0	6.0	4.0	0.90	20	32	1
.75	4.5	4.5	6.0	6.0	0.90	20	32	1
1.5	4.5	4.5	3.0	3.0	---	---	---	---

APPENDIX VIII.

(continued)

C. Jefferson City Dolomite

Burden (in.)	Length (in.)	Spacing (in.)	L/B	S/B	L_1/L	Angle x (deg.)	Angle y (deg.)	Crater Form
.5	0.5	1.0	1.0	2.0	1.0	25	36	2
.5	0.5	1.5	1.0	3.0	1.0	28	35	1
.5	3.0	2.0	6.0	4.0	1.0	18	38	2
.5	3.0	2.5	6.0	5.0	1.0	20	37	1
.5	3.0	3.0	6.0	6.0	1.0	20	35	1

APPENDIX IX.

EXPERIMENTAL DATA FOR SINGLE CHARGES

Note: Tested with 10-gr MDF

Material	Burden (in.)	Length (in.)	L/B	L_1/L	Angle x (deg.)	Angle y (deg.)
Plexiglas	.5	3.0	6.0	.90	40	45
Mortar	.75	1.5	2.0	.71	20	35
Mortar	.75	4.5	6.0	.89	20	37
Dolomite	1.0	3.0	3.0	1.0	24	36

REFERENCES

1. ANDERSON, O. (1952). Blast Hole Burden Design--Introducing a Formula; Australasian Institute of Mining and Metallurgy, Proceeding Nos. 166-167; September and December.

2. ASH, R. L., and CASQUINO, W. T. (1967). Conical Stress-Waves Generated by Explosive Charges; Society of Mining Engineers of AIME, Preprint No. 67FM45.

3. ASH, R. L. (1963). The Mechanics of Rock Breakage, Parts I, II and IV; Pit and Quarry, Vol. 56, Nos. 2, 3 and 5; August, September and November.

4. ASH, R. L. (1961). Drill Pattern and Initiation-Timing Relationships for Multiple-Hole Blasting; Quarterly, Col. School of Mines, Vol. 56, No. 1.

5. AUSTIN, C. F., COSNER, L. N., and PRINGLE, J. K. (1965). Shock Wave Attenuation in Elastic and Inelastic Rocks; Proceedings, 7th Symposium on Rock Mechanics, Penn. State Univ., June.

6. CASQUINO, W. T. (1965). The Development of Conical Stress Forms by Explosive Charges; Unpublished M.S. Thesis, Univ. of Mo. at Rolla.

7. CLARK, G. B. (1966). Blasting and Dynamic Rock Mechanics; Proceedings, 8th Symposium on Rock Mechanics, Univ. of Minn.

8. CLARK, G. B., and ROLLINS, R. R. (1965). Simplified Explosives Calculations; Eng. and Min. Journal, Vol. 166, No. 6, June.

9. COOK, M. A. (1958). The Science of High Explosives; ACS Monograph 139, Reinhold Publications Co., New York.

10. DEATHERAGE, J. H., Jr. (1966). The Development of the Sonic Pulse Technique and Its Comparison with Conventional Static Method for Determining the Elastic Moduli Rock: Unpublished M.S. Thesis, Univ. of Mo. at Rolla.

11. DUVALL, W. I., and ATCHISON, T. C. (1957). Elastic Waves in Layered Media; McGraw Hill Book Co., Inc., New York.

12. Ensign-Bickford Company (1960). Primacord Detonating Fuse Catalog, 4th Printing.

13. GRANT, C. H. (1965). Design of Open Pits; Proceedings, 7th Symposium on Rock Mechanics, Penn. State Univ., June.

14. HAAS, C. J. (1964). Fractures Produced in the Neighborhood of Openings by Impulsive Loads; Unpublished M.S. Thesis, Col. School of Mines, Golden.

15. Handbook of Chemistry and Physics (1961). Forty-third Edition Chemical Rubber Publishing Co., Cleveland, Ohio.

16. KOCHANOWSKY, B. J. (1957). Principles of Blasting; Univ. of Mo. School of Mines and Metallurgy, Rolla, Bulletin Technical Series No. 94.

17. KOLSKY, H. (1963). Stress Waves in Solids; Dover Publications, Inc., New York.

18. LANGEFORS, U., SJOLIN, T., and PEDERSON, A. (1965). Fragmentation in Rock Blasting; Proceedings, 7th Symposium on Rock Mechanics, Penn. State Univ., June.

19. LANGEFORS, U., and KIHLSTROM, B. (1963). Rock Blasting; John Wiley and Sons, inc., New York.

20. LIVINGSTON, C. W. (1960). Explosive Research Applied to Mine and Quarry Blasting; Min. Eng., Vol. 12, No. 1.

21. MURPHY, G. (1950). Similitude in Engineering; The Ronald Press Co., New York.

22. PEARSE, G. E. (1955). Rock Blasting - Some Aspects on the Theory and Practice; Mine and Quarry Eng., Vol. 21, No. 1, January.

23. Regal Plastic Supply Co. (1963). Catalog; Englewood, Denver, Colorado.

24. SLYKHOUSE, T. E. (1965). Empirical Methods of Correlating Explosive Cratering Results; Proceedings, 7th Symposium on Rock Mechanics, Penn. State Univ., June.

25. STARFIELD, A. M. (1966). Strain Wave Theory in Rock Blasting; Proceedings, 8th Symposium on Rock Mechanics, Univ. of Minn.

VITA

Calvin J. Konya was born on June 23, 1943, in Cleveland, Ohio. He received his primary and secondary education in Cleveland. He has received his college education from Case Institute of Technology in Cleveland, Ohio; the College of Advanced Science in Canaan, New Hampshire; John Carroll University in Cleveland, Ohio and the University of Missouri at Rolla. As an undergraduate, he received the Don B. McCloud Memorial Fund Scholarship for two years. He received his Bachelor of Science Degree in Mining Engineering in August, 1966.

He has been enrolled as a graduate student at the University of Missouri at Rolla since September, 1966. During his first year of graduate study, he held a graduate assistantship in the Department of Mining Engineering. He is presently studying under a National Defense Education Act Grant.